



Published in final edited form as:

Nature. 2021 February ; 590(7844): 157–162. doi:10.1038/s41586-020-03075-w.

Mechanism of EBV inducing anti-tumour immunity and its therapeutic use

Il-Kyu Choi^{1,2,9}, Zhe Wang^{1,2,9}, Qiang Ke^{1,3}, Min Hong^{1,4}, Dereck W. Paul Jr^{1,8}, Stacey M. Fernandes¹, Zhuting Hu¹, Jonathan Stevens⁵, Indira Guleria^{2,5}, Hye-Jung Kim^{6,7}, Harvey Cantor^{6,7}, Kai W. Wucherpfennig^{6,7}, Jennifer R. Brown^{1,2}, Jerome Ritz^{1,2}, Baochun Zhang^{1,2,6,*}

¹Department of Medical Oncology, Dana-Farber Cancer Institute, Boston, MA, USA

²Department of Medicine, Harvard Medical School, Boston, MA, USA

³Department of Diagnostics, School of Medicine, Hangzhou Normal University, Hangzhou, Zhejiang, China

⁴Department of Medical Oncology, The First Affiliated Hospital of Kunming Medical University, Kunming, Yunnan, China

⁵Clinical Laboratory Division, Brigham and Women's Hospital, Boston, MA, USA

⁶Department of Cancer Immunology and Virology, Dana-Farber Cancer Institute, Boston, MA, USA

⁷Department of Immunology, Harvard Medical School, Boston, MA, USA

⁸Present address: University of California, San Francisco, School of Medicine, San Francisco, CA, USA

⁹These authors contributed equally: Il-Kyu Choi, Zhe Wang

Summary

Tumour-associated antigens (TAAs) comprise a large collection of non-mutated cellular antigens recognized by T cells in human and murine cancers. Their potential as immunotherapy targets has been explored for over two decades¹, yet the genesis of TAA-specific T cells remains elusive. While tumour cells may be an important source of TAAs for T cell priming², several recent studies suggest that infection with some viruses including Epstein-Barr virus (EBV) and influenza virus

Users may view, print, copy, and download text and data-mine the content in such documents, for the purposes of academic research, subject always to the full Conditions of use:http://www.nature.com/authors/editorial_policies/license.html#terms Reprints and permissions information is available at www.nature.com/reprints.

*Correspondence and requests for materials should be addressed to B.Z. (baochun_zhang@dfci.harvard.edu).

Author Contributions: I.K.C. and B.Z. planned and coordinated the overall research; I.K.C. and Z.W. designed and performed experiments and data analysis with Q.K., M.H. and D.W.P.; S.M.F., J.R.B. and J.R. provided CLL patient samples; Z.H. provided technical advice; J.S. and I.G. characterized CLL patient samples; H.J.K., H.C., K.W.W., J.R.B. and J.R. provided scientific and experimental advice, and edited the manuscript; I.K.C. and B.Z. interpreted the results and wrote the manuscript; B.Z. conceived and supervised the project.

The authors declare competing financial interests: I.K.C., Z.W. and B.Z. are inventors on patent applications which cover parts of this work; Z.H. is a current employee of ElevateBio.

Publisher's note: Springer Nature remains neutral with regard to jurisdictional claims in published maps and institutional affiliations. Readers are welcome to comment on the online version of the paper.

can elicit T cell responses against abnormally expressed cellular antigens that function as TAAs^{3,4}. However, the cellular and molecular basis of such responses remains undefined. Here, we show that expression of the EBV signaling protein LMP1 in B cells provokes T cell responses to multiple TAAs. LMP1 signaling leads to overexpression of many cellular antigens previously shown to be TAAs, their presentation on MHC-I and -II (mainly through the endogenous pathway), and the upregulation of costimulatory ligands CD70 and OX40L, thereby inducing potent cytotoxic CD4⁺ and CD8⁺ T cell responses. These findings delineate a novel mechanism of infection-induced anti-tumour immunity. Furthermore, by ectopically expressing LMP1 in patient tumour B cells and thereby empowering them to prime T cells, we develop a general approach for rapid production of autologous cytotoxic CD4⁺ T cells against a broad array of endogenous tumour antigens, such as TAAs and neoantigens, for treating B-cell malignancies. This work stresses the need to revisit classical concepts concerning viral and tumour immunity, which will be critical to fully understand the impact of common infections on human health and to improve the rational design of immune approaches for cancers.

EBV, a B-cell tropic virus infecting > 90% of humans, is rapidly controlled on initial infection by T cell surveillance; thereafter, the virus establishes a lifelong latent infection in the host. When surveillance fails, fatal lymphoproliferation and lymphomagenesis ensue⁵. Recent studies in mouse models revealed a central role for LMP1 in both the surveillance and transformation of EBV-infected B cells *in vivo*: Constitutive or inducible expression of LMP1 in mouse B cells induced potent T cell responses which in turn eliminated LMP1⁺ B cells; upon T cell depletion LMP1 drove rapid B cell proliferation and lymphomagenesis^{6,7}. Our analysis of the T cell response showed that both CD4⁺ and CD8⁺ T cells exhibit typical cytotoxic T cell (CTL) phenotype and function. Our data further indicated that LMP1⁺ B cells upregulate costimulatory ligands and drive the differentiation and expansion of Eomesodermin (Eomes)⁸-programmed CD4 CTLs via CD70- and OX40 ligand (OX40L)-mediated costimulation, and of CD8 CTLs via CD70, OX40L, as well as 4-1BB ligand (4-1BBL)⁹. Using Eomes- and Perforin-deficient CD4 cells, we confirmed Eomes-dependent differentiation and perforin-granzyme pathway mediated cytotoxic function of the CD4 CTLs (Extended Data Fig. 1). Yet, the antigens targeted by T cells in the LMP1 mouse models remain unidentified.

T cells recognize LMP1-induced cell antigens

Our attempts to identify LMP1-derived peptides as potential T cell targets were unsuccessful⁶. Moreover, we found that T cells from mice constitutively expressing LMP1 in B cells (*CD19-cre;LMP1^{floxSTOP}* mice, hereafter termed *CL* mice), recognized and killed B cells expressing wild-type LMP1, but not those expressing a signaling-dead LMP1 mutant with just three amino acid changes (LMP1^{TM1m}; Fig. 1a). These findings argue against LMP1-derived epitopes as major targets of T cells, in agreement with human studies suggesting the immunostimulatory LMP1 protein evolved to avoid T cell recognition^{5,10}.

Analysis of the T cell receptor (TCR) V β repertoire on CD4 (excluding Foxp3⁺ regulatory T cells (Tregs)) and CD8 cells in *CL* mice revealed that (1) during the acute phase of the immune response both CD4 and CD8 cells mounted a grossly polyclonal response (although

a few V β TCRs showed some degrees of enrichment, cytotoxicity was not restricted to them); and (2) there was no clonal deletion of any V β TCR afterwards (Extended Data Fig. 2). These findings suggest that T cells target a wide range of antigens, and not a superantigen¹¹.

LMP1 has been characterized as a functional analog of constitutively active CD40, as they share many signaling pathways in B cells¹². Both LMP1 and CD40 signaling upregulated major histocompatibility complex (MHC)-I and -II in B cells (Fig. 1b), and were previously shown to enhance presentation of endogenously expressed antigens^{10,13}. We therefore reasoned that T cells might target certain cellular antigens presented by LMP1⁺ B cells, and some of these antigens might also be shared with CD40-activated B cells. Indeed, CD4 and CD8 cells from *CL* mice lysed CD40-activated wild-type (WT) B cells (CD40-B cells), but not naive B cells (Fig. 1c); CD4 cell-mediated lysis was partially suppressed by blocking MHC-II recognition (Fig. 1d). A proliferation assay further confirmed recognition of CD40-B cells by effector CD4 cells (excluding Tregs) in an MHC-II-restricted manner (Fig. 1e). These findings, along with the lack of killing of naive or LPS-activated B cells (Fig. 1a, c), suggest the T cells target certain LMP1-induced cellular antigens (some of which are also inducible by the analogous CD40 signaling), but not “resting B cell antigens”, and not all “activated B cell antigens”.

In accord with the *in vitro* finding, the T cell response elicited by LMP1⁺ B cells also led to marked depletion of *in vivo* CD40-activated B cells, such as germinal center B cells, as found in inducible LMP1-expressing *CD19-cre^{ERT2};LMP1^{flSTOP} (ERT2-CL)* mice⁷ (Extended Data Fig. 3; Supplementary Discussion). Although our data indicate LMP1⁺ B cells and CD40-B cells present some shared cellular antigens, we found that CD40-B cells exhibited little induction of OX40L and no induction of CD70, and upon co-culture with naive CD4 cells led to no generation of Eomes⁺ CD4 CTLs, in stark contrast to LMP1⁺ B cells (Extended Data Fig. 4). Hence, LMP1 signaling is unique and distinct from that of CD40 in its ability to elicit CD4 CTL response.

LMP1-induced TAAs are targets of T cells

We sought to identify LMP1-induced cellular antigens. As LMP1 is a key oncoprotein for EBV-driven tumorigenesis¹⁴, we hypothesized that LMP1-induced cellular proteins targeted by T cells would be tumour-associated antigens (TAAs). Gene expression analysis identified many LMP1-induced genes encoding proteins known to function as TAAs in humans and/or mice; as expected, some of them are also upregulated in CD40-B cells (Fig. 2a). We chose two of these TAAs—Survivin and Ephrin type-A receptor 2 (EphA2), whose epitopes and restricting MHC-I alleles have been well characterized—to validate T cell responses in the LMP1 mouse models. We confirmed the overexpression of Survivin and EphA2 proteins in LMP1⁺ B cells (Fig. 2b). By tetramer staining we detected clear CD8 responses against both TAAs in *CL* neonates (on a (BALB/c \times C57BL/6)F1 (CB6F1) background) around the peak of T cell response⁹, compared to littermate controls (Fig. 2c). EBV infection usually occurs in childhood or young adulthood and begins in a small fraction of B cells, and these dynamics are better modeled in *ERT2-CL* mice⁷. Therefore, we tested whether TAA-specific CD8 responses can also be efficiently generated in these mice

at young adulthood (6–8 weeks old) when immune tolerance to self has been well established. Indeed, Survivin- and EphA2-specific CD8 responses were readily detected in *ERT2-CL* mice (on the same CB6F1 background) around the peak of T cell response, but not in littermate controls (Fig. 2d). By contrast, no CD8 response to an irrelevant LCMV antigen could be detected by the antigen-specific tetramer (Extended Data Fig. 5a, b), further attesting to the TAA-directed responses in LMP1 mice. Moreover, TAA-specific CD8 cells exhibited an antigen-experienced CD44^{high} phenotype (Extended Data Fig. 5c), and their dynamics paralleled LMP1⁺ B cells (Fig. 2e), in line with the latter being both stimulators and targets of T cells⁹. We also generated *ERT2-CL* mice on a pure C57BL/6 (B6) background and confirmed the Survivin- and EphA2-specific CD8 responses by the tetramers (Extended Data Fig. 5d).

Because no class II epitopes from the list of LMP1-induced TAAs have been characterized in the mouse system, we took different approaches to demonstrate that TAAs expressed in LMP1⁺ B cells can be naturally processed and presented on MHC-II as targets of CD4 cells. First, we showed that CD4 cells primed by LMP1⁺ B cells displayed MHC-II–dependent recognition of two LMP1-negative B-cell lymphoma lines 775 and 773, as measured by CD4 cell proliferation assay (Fig. 2f), indicating they target certain shared TAAs. Second, we tested whether an ectopically transfected TAA—Tyrosinase-related protein 1 (Trp1)—can be presented by LMP1⁺ B cells on MHC-II to activate naive CD4 cells that express a TCR specific to a class II (I-A^b)–restricted Trp1 epitope¹⁵. An LMP1-driven B-cell line 1019 (I-A^b⁺; no expression of Trp1 unless ectopically transfected with Trp1 mRNA) and a control *CIITA*^{-/-} subline (MHC-II⁻) were used (Fig. 2g). The CD4 cells upregulated the activation marker CD69 upon co-culture with Trp1-transfected 1019 cells, but not with untransfected 1019 cells or transfected MHC-II⁻ variants (Fig. 2h), indicating TCR recognition of the Trp1 epitope presented on MHC-II of transfected 1019 cells.

It is well established that antigenic proteins expressed within antigen-presenting cells (APCs) are generally processed endogenously for MHC-I presentation. Several studies have also shown that B cells, including EBV-transformed B-lymphoblastoid cells (LCLs), can present a wide range of endogenously expressed antigens from diverse cellular compartments on MHC-II, also through the endogenous pathway^{16–18}. Nonetheless, it is possible that some antigens are released into extracellular milieu followed by uptake and processing as exogenous antigens (exogenous pathway). To assess by which route(s) LMP1⁺ B cells present the endogenously expressed Trp1 on their MHC-II, we used culture systems depicted in Fig. 2i. In Culture 1, Trp1 epitope peptide may be presented on MHC-II through the endogenous pathway; in Culture 2, it may only be presented through the exogenous pathway. Marked CD69 upregulation was detected in Trp1-specific CD4 cells in Culture 1 but not Culture 2 (Fig. 2i), indicating that the Trp1 epitope is presented on MHC-II of LMP1⁺ B cells predominantly through the endogenous pathway.

Collectively, these results show that LMP1 signaling in B cells leads to overexpression of multiple TAAs and their presentation on MHC-I and -II, mainly through the endogenous pathway. Together with LMP1-induced costimulatory ligands, in particular CD70 and OX40L⁹, this provokes cytotoxic CD4 and CD8 T cell responses to these TAAs (see schematic in Extended Data Fig. 6). This conclusion is further supported by the observation

that Trp1-transfected 1019 cells sufficed to prime naive Trp1-specific CD4 cells into CD4 CTLs *in vitro* (Fig. 2j).

The LMP1-induced TAA-specific T cell responses appear to cause no discernible harm to hosts. Histological examination of various tissues in LMP1 mice after the T cell contraction revealed no pathological changes (Extended Data Fig. 7), and both *CL* and *ERT2-CL* mice exhibited no noticeable illness over a 1.5-year observation period.

An LMP1-based CD4 CTL therapeutic approach

Based on these discoveries, we envisioned exploiting LMP1 to develop immune approaches for treating cancers. Of particular interest was to develop a CD4 CTL therapy for B-cell malignancies, as (1) our previous work showed superior therapeutic efficacy of CD4 CTLs over CD8 CTLs in LMP1-driven B-cell lymphoma models⁹, and (2) many B-cell tumours in patients, including > 70% of diffuse large B-cell lymphomas and classical Hodgkin lymphomas, completely lose MHC-I expression^{19,20} and thus cannot be targeted by CD8 CTLs. We conceived that ectopically expressing LMP1 in patient tumour B cells should make them (i) enhance presentation of endogenous antigens, such as TAAs and neoantigens, on MHC-II, and (ii) concurrently upregulate costimulatory ligands, particularly CD70 and OX40L, thereby eliciting CD4 CTLs against these tumour antigens. CD4 CTLs generated in this fashion should be able to kill unmodified tumour B cells that express the same antigens (see schematic in Extended Data Fig. 8), and thus can be used for adoptive cell therapy (ACT).

We validated this therapeutic concept using the murine (BALB/c-derived) B-cell lymphoma model A20, an aggressive, poorly immunogenic tumour, in part due to its lack of costimulatory ligands²¹. As expected, LMP1 expression in A20 cells led to upregulation of MHC-II and costimulatory ligands, including CD80 for T cell activation and more importantly, CD70 and OX40L capable of driving cytotoxic CD4 differentiation. The upregulation of these molecules depended on LMP1 signaling, as it was not observed in LMP1^{TM1m}-transduced A20 cells (Fig. 3a). Cultivating naive CD4 cells with LMP1-transduced A20 cells, but not LMP1^{TM1m}-transduced A20 cells, for 6–7 days led to marked expansion of the CD4 cells (Fig. 3b), and a significant fraction of them expressed Eomes (Fig. 3c). Importantly, the primed CD4 cells displayed potent cytotoxicity to unmodified A20 cells, but not control naive B cells (Fig. 3d). The cytotoxicity was abolished when A20 cells were abrogated of MHC-II expression by knockout of *CIITA* (Fig. 3e, f), indicating that the CD4 CTLs kill A20 cells by recognizing their endogenous tumour antigens presented on MHC-II. Furthermore, the CD4 CTLs exhibited MHC-II-dependent killing of a different BALB/c-derived B-cell lymphoma/leukaemia line BCL1 (Extended Data Fig. 9a), indicating the CD4 repertoire targets TAAs shared by multiple tumours.

We next evaluated therapeutic efficacy of the CD4 CTLs against pre-established A20 tumours in syngeneic hosts (Fig. 3g). Upon adoptive transfer, the CD4 CTLs markedly limited tumour growth, whereas naive CD4 cells had no effect (Fig. 3h). Adoptive CD4 CTLs infiltrated/accumulated in the tumours at significantly higher frequency and number, compared to adoptively transferred naive CD4 or activated Th0 type CD4 cells (Fig. 3i and

Extended Data Fig. 9b). Furthermore, the intra-tumoural adoptive CD4 CTLs at day-8 post-transfer maintained a cytotoxic phenotype, as evidenced by Granzyme B and Perforin expression (Fig. 3j). These data indicate that CD4 CTLs primed by LMP1-transduced A20 cells, upon adoptive transfer, can accumulate in the A20 tumours and mediate direct tumour killing by targeting TAAs and possibly neoantigens expressed in A20 cells, resulting in significant anti-tumour efficacy. Nevertheless, we were concerned that the activity of adoptive CD4 CTLs might be negatively regulated by immune checkpoint mechanisms, particularly the PD-1 pathway. A20 cells are known to express high levels of the PD-1 ligand PD-L1²¹, and we found that the intra-tumoural adoptive CD4 CTLs expressed substantial levels of PD-1 (Fig. 3k). PD-1 blockade markedly improved anti-tumour efficacy, inducing apparent cure in more than half of mice treated with the combination therapy (Fig. 3l, m). Of note, no sign of toxicity was observed in mice receiving CD4 CTL or the combination therapy (data not shown). Taken together, this murine B-cell lymphoma model demonstrates an LMP1-based approach for rapid production of therapeutic CD4 CTLs for B-cell malignancies, and their use as ACT *in vivo*, potentially in combination with checkpoint blockade.

Production of human CD4 CTLs

To test whether the LMP1-based CD4 CTL production approach can translate to humans, we chose to experiment on chronic lymphocytic leukaemia (CLL), a prevalent B-cell malignancy in adults, in which CLL cells and autologous CD4 cells are both readily accessible in peripheral blood. Moreover, the poor immunogenicity of CLL cells (they present multiple TAAs on HLA-II²² but lack expression of costimulatory ligands) makes them particularly suitable for demonstrating LMP1-induced immunogenicity. We identified an efficient method of gene delivery into primary CLL cells (without any pre-stimulation) using mRNA nucleofection (Fig. 4a). LMP1 expression in CLL cells led to further increase in HLA-II and more importantly, marked upregulation of costimulatory ligands including CD80, CD70 and OX40L (Fig. 4b, c), as it did in mouse tumour B cells (Fig. 3a). As expected, stimulation of autologous CD4 cells with LMP1-CLL cells produced CD4 CTLs that lysed parental CLL cells in an HLA-II-restricted fashion (indicative of targeting CLL antigens presented by HLA-II; Fig. 4d). These results not only establish the feasibility of using the LMP1-based approach to produce autologous CD4 CTLs targeting patient tumour B cells, but also demonstrate that LMP1 executes essentially identical immunostimulatory functions in mice and humans.

However, the immune status of the CD4 source cells for CD4 CTL generation were different in the mouse and human experiments. In the mouse A20 experiments, naive CD4 cells were used. In the human CLL studies, the CD4 cells were from patient peripheral blood, where they would have been pre-exposed to tumour antigens. A previous study identified large numbers of HLA class II-presented TAA epitopes in CLLs, and detected T cell responses to several of them (after pre-stimulation/amplification) in peripheral blood mononuclear cells (PBMCs) from CLL patients, but not from healthy donors²². We therefore predicted that the CLL-reactive CD4 CTLs produced by our approach are most likely derived from antigen-exposed effector/memory type CD4 cells. Using an activation-induced marker assay, we demonstrated, in three CLL cases, that approximately 4–9% of effector/memory CD4 cells

from their PBMCs were activated by LMP1-CLL cells, as evidenced by co-expression of CD69 and CD40L (Fig. 4e and Extended Data Fig. 10a, b). We next used previously identified HLA-II epitopes from three CLL TAAs—Cathepsin H (CTSH), Transferrin receptor (TFRC) and Vesicle-associated membrane protein 2 (VAMP2)—to confirm that the CD4 cells produced by stimulation with LMP1-CLL cells target these antigens. Interferon (IFN)- γ enzyme-linked immunospot (ELISPOT) analysis showed that reactivity to at least one of these TAAs could be detected in the CD4 products from 4 of 5 CLL patients (Fig. 4f and Extended Data Fig. 10c, e). In one patient, an HLA-II blocking experiment confirmed the HLA-II-restriction of the TAA response (Fig. 4f, Pt. 10). Parallel analysis of unstimulated CD4 cells from two patients detected no response to any of these TAAs (Extended Data Fig. 10d). This suggests that patient PBMCs harbor CD4 cells to individual TAAs at low frequencies²², and that stimulation with LMP1-CLL cells can potently activate/expand them into CD4 CTLs.

Discussion

Our study in mouse models shows that expression of LMP1 in B cells provokes T cell responses to multiple TAAs; it also illustrates the molecular processes leading to such responses. These findings indicate that in humans, EBV infection elicits T cell responses not only against viral antigens⁵, but also against a wide range of TAAs induced by LMP1 (and perhaps by other EBV signaling molecules). In this regard, the present work provides an underlying mechanism for the previous observation suggesting that stimulation by autologous EBV-LCLs leads to generation of human cytotoxic CD4 cells recognizing shared TAAs³. Similarly, Survivin- and other TAA-specific T cells detected in patients receiving LCL-stimulated T cells to treat EBV-associated lymphomas might have been generated by the LMP1-mediated mechanism, not necessarily by epitope spreading²³. Future studies to identify TAAs expressed by EBV-infected/transformed B cells and demonstrate their recognition by T cells in EBV-infected individuals are warranted. Subjects at early stages of infection, in which mysterious “bystander T cells” are reportedly dominant over EBV-specific T cells^{24,25}, may be particularly suitable for this type of study. Furthermore, longitudinal study of TAA-specific T cells in these subjects may lead to insights into anti-tumour immunity against EBV-related and other cancers.

Exploiting LMP1, we develop a unique approach to produce CD4 CTLs for treating B-cell malignancies. This enables targeting a wide range of endogenous tumour antigens, such as TAAs and neoantigens, without the need to identify them in each patient. CD4 CTL responses to TAAs have been demonstrated in the present work; responses against neoantigens will be investigated in future studies. Of note, additional data in our CLL study and from literature indicate that pre-existing EBV immunity in patients will not impede the use of LMP1-based approach to produce therapeutic CD4 CTLs (Supplementary Discussion). Encouraged by the preclinical study in A20 model, our efforts to translate the CD4 CTL-based ACT to clinical testing as a standalone therapy and in combination with checkpoint blockade (Supplementary Discussion) are underway.

Besides direct cytotoxicity, CD4 CTLs may exert helper functions via interaction with APCs to enlist other immune effectors, such as CD8 cells, tumouricidal macrophages and NK

cells, into tumour immunity. Therefore, CD4 CTLs hold therapeutic value for not only MHC-II positive but also MHC-II negative tumours²⁶, as indeed exemplified by some recent preclinical and clinical studies (Supplementary Discussion). Future efforts to develop multiantigen-targeted CD4 CTL approaches for these latter tumours should be rewarding.

METHODS

No statistical methods were used to predetermine sample size. The experiments were not randomized, and investigators were not blinded to allocation during experiments and outcome assessment, except where stated otherwise.

Mice.

C57BL/6 (B6), *CD4-cre*, *CD19-cre*, *CD19-cre^{ERT2}*, *CIITA^{-/-}*, *Eomes^{F/F}*, *Foxp3^{DTR/GFP}*, *Prf1^{-/-}*, *Rag1^{-/-}B^W* tyrosinase-related protein 1 (Trp1) T cell receptor (TCR) transgenic (Trp1 mice) and *YFP^{flSTOP}* mice (all on a B6 background), and BALB/c (CD45.2⁺) and CD45.1⁺ congenic mice were obtained from the Jackson Laboratory. The *LMP1^{flSTOP}* allele on a BALB/c background has been described⁶, and that on a B6 background was generated by backcrossing to B6 mice. *CD19-cre;LMP1^{flSTOP}* (CL) mice on a (BALB/c × B6)F1 (CB6F1) background have been described⁶. Homozygous *CD19-cre^{ERT2}* mice were crossed with *LMP1^{flSTOP}* heterozygous mice on the BALB/c or B6 background to generate *CD19-cre^{ERT2};LMP1^{flSTOP}* (*ERT2-CL*) and *CD19-cre^{ERT2}* (*ERT2-C*) control mice on the CB6F1 or B6 background. To activate Cre^{ERT2}, mice were treated with 4 mg tamoxifen (Sigma; dissolved in sunflower oil) by intragastric gavage. *Foxp3^{DTR/GFP};CL* mice on the CB6F1 background were generated by crossing *CD19-cre;Foxp3^{DTR/GFP}* to *LMP1^{flSTOP}* mice on the BALB/c background. Only male *Foxp3^{DTR/GFP};CL* mice were used in experiments (in males, all Foxp3⁺ CD4 Tregs express the GFP reporter). Both sexes of all other strains were used (for *in vivo* work, the recipient and donor mice were sex-matched). The experiments that involve gene-modified mice and littermate controls younger than 21 days were randomized and blinded; their genotypes were determined only after the experiments and data analyses were completed. All mice were bred and maintained in the animal facilities at the Dana-Farber Cancer Institute (DFCI), under specific pathogen-free conditions (with a 12 h light-dark cycle at temperature of 21–23°C and humidity of 35–55%), and used at the ages of 6–12 weeks, except where indicated otherwise. All animal experiments were conducted per protocols approved by the DFCI Institutional Animal Care and Use Committee.

Patient samples.

Heparinized blood and plasma samples were obtained from untreated chronic lymphocytic leukaemia (CLL) patients at the time of diagnosis (no other selection criteria), under prospectively consented DFCI IRB approved tissue bank protocols. Patient peripheral blood mononuclear cells (PBMCs) were isolated by Ficoll/Paque (GE Healthcare) density gradient centrifugation and then separated into CD19-positive and CD19-negative populations using anti-CD19 microbeads (Miltenyi Biotec). Positively selected cells were ~95% of CD19⁺CD5⁺ CLL B cells as determined by fluorescence-activated cell sorting (FACS). Negatively selected cells were further FACS-sorted into CD4⁺CD25^{low/-} T cells (excluding CD56⁺ and TCRγδ⁺ cells), effector/memory subsets (excluding CD45RA⁺CCR7⁺ naive

subset) or CD14⁺ monocytes. These cells were used fresh or cryopreserved (with human serum (Gemini Bioproduct) containing 10% DMSO) for later use. Plasma samples were stored at -80°C until analyzed.

Flow cytometry.

Single-cell suspensions were treated with Fc block (mouse or human TruStain FcX; Biolegend) and then stained with the following monoclonal antibodies specific for mouse B220 (RA3-6B2, 1:200), CD3 (17A2, 1:100), CD4 (GK1.5, 1:400), CD8 (53-6.7, 1:400), CD11b (M1/70, 1:200), CD19 (6D5, 1:200), CD25 (7D4, 1:200 and PC61, 1:200), CD38 (90, 1:300), CD43 (S7, 1:200), CD44 (IM7, 1:160), CD45.1 (A20, 1:100), CD49b (DX5, 1:200), CD62L (MEL-14, 1:400), CD69 (H1.2F3, 1:100), CD70 (FR70, 1:100), CD80 (16-10A1, 1:200), OX40L (RM134L, 1:100), Fas (Jo2, 1:800), Gr-1 (RB6-8C5, 1:200), H-2K^b (AF6-88.5, 1:200), I-A^b (AF6-120.1, 1:800), I-A^d (AMS-32.1, 1:800), PD-1 (RMP1-30, 1:100), TER-119 (TER-119, 1:200), TCR β (H57-597, 1:400), TCR V β 5.1/2 (MR9-4, 1:200), TCR V β 11 (RR3-15, 1:200), TCR V β 12 (MR11-1, 1:200), Granzyme B (NGZB, 1:100), Perforin (eBioOMAK-D, 1:20), Foxp3 (FJK-16s, 1:50), Eomes (Dan11mag, 1:50), human CCR7 (G043H7, 1:100), CD3 (SK7, 1:400), CD4 (OKT4, 1:400), CD5 (UCHT2, 1:200), CD8 (SK1, 1:200), CD14 (M5E2, 1:100), CD19 (HIB19, 1:200), CD25 (M-A251, 1:400), CD40L (24-31, 1:100), CD45RA (HI100, 1:100), CD56 (HCD56, 1:400), CD69 (FN50, 1:100), CD70 (113-16, 1:100), CD80 (2D10, 1:200), Fas (DX2, 1:100), HLA-II (-DR, -DP, -DQ; Tü39, 1:3200), OX40L (11C3.1, 1:100) and TCR $\gamma\delta$ (B1, 1:400) from BD Biosciences, Biolegend, eBioscience or Invitrogen. Topro3 (Invitrogen) or eFluor 506 (eBioscience) staining was employed to exclude dead cells. Intracellular staining for Granzyme B, Perforin, Foxp3 and Eomes was done with the Foxp3 staining buffer set (eBioscience). For Granzyme B and Perforin staining of *in vitro* generated CD4⁺ cytotoxic T cells (CD4 CTLs), cells were re-stimulated for 5 h with phorbol 12-myristate 13-acetate (PMA, 0.1 μ M; Sigma) and ionomycin (1 μ M; Sigma), and supplemented with Brefeldin A (1:1000; Biolegend) in the last 3 h before intracellular staining. The TCR V β repertoire was analyzed with the mouse V β TCR screening panel (BD Biosciences) according to the manufacturer's instructions. All samples were acquired on a FACSCanto II or LSRFortessa using FACSDiva v8.0.1 software (all BD Biosciences) and analyzed by FlowJo v10.0.7 software (Tree Star). FACS sorting was performed using a FACSARIA II with FACSDiva v8.0.1 software (both BD Biosciences). In all mouse T cell sorting experiments, the CD1d tetramer (NIH tetramer facility) was used to exclude natural killer T cells.

Culture of cell lines.

The mouse lymphoma cell lines driven by LMP1 (line 1019; I-A^{b+}) or Bcl6 (lines 773 and 775; both I-A^{b+}), established by us^{6,27}, were cultured in DMEM medium (Gibco) supplemented with 10% FBS (Sigma), 100 IU/ml penicillin (Gibco), 10 mM HEPES (Corning), 1 \times non-essential amino acids (Corning), 1 mM sodium pyruvate (Gibco) and 50 μ M β -mercaptoethanol (Sigma). The 1019, 773 and 775 cells were authenticated by Western blotting and/or PCR genotyping. The A20 and BCL1 mouse lymphoma cell lines (both I-A^{d+}, I-E^{d+}), purchased from ATCC, were maintained in RPMI 1640 medium (Gibco) supplemented with 10% (for A20 cells) or 15% (for BCL1 cells) FBS, 2 mM L-glutamine (Gibco), 100 IU/ml penicillin and 50 μ M β -mercaptoethanol. The B16-F10 mouse

melanoma and HEK293T cell lines, obtained from ATCC, were cultured in DMEM medium supplemented with 10% FBS and 100 IU/ml penicillin. Because A20, BCL1, B16-F10 and HEK293T cells were purchased from ATCC, no additional authentication was performed. All the cells were cultured at 37°C in 5% CO₂, and tested negative for mycoplasma contamination.

Mouse B cell isolation and treatment.

Mouse splenic B cells were purified by CD43-depletion using magnetic-activated cell sorting (MACS; Miltenyi Biotec) according to the manufacturer's protocol. To turn on LMP1 expression *in vitro*, B cells isolated from *LMP1^{flSTOP}* mice were treated with TAT-Cre as described previously²⁸. For CD40 activation, purified B cells were cultured in the presence of 1 µg/ml anti-CD40 (HM40-3; Biolegend). Two days after TAT-Cre transduction or CD40 stimulation, cells were analyzed by FACS or used in other experiments. All B cells were cultured in DMEM medium supplemented with 10% FBS, 100 IU/ml penicillin, 10 mM HEPES, 1× non-essential amino acids, 1 mM sodium pyruvate and 50 µM β-mercaptoethanol.

Retroviral constructs and transduction.

cDNA encoding wild-type LMP1 or a signaling-defective mutant LMP1^{TM1m} was previously cloned into the MSCV-IRES-GFP or MSCV-Puro retroviral vector⁹. The respective retroviral vector was co-transfected with Eco (pCL-Eco) or VSVG packaging plasmids (pCMV-VSVG and pKat) into HEK293T cells. After 48 h, viral supernatants were harvested, passed through a 0.45-µm filter, and then used to infect cells immediately or stored at -80°C for later use. Mouse B cells were transduced with Eco-pseudotyped retroviruses carrying GFP or Puro as previously described⁹. For transduction of A20 cells, cells were spin-infected with VSVG-pseudotyped retroviruses carrying GFP (at 300 g, 25°C for 3 h in the presence of 10 µg/ml polybrene (Sigma)), and 48 h later GFP⁺ cells were sorted by FACS.

Generation of *CIITA* knockout lymphoma sublines by CRISPR-Cas9.

A single-guide RNA (sgRNA) sequence targeting exon 2 or exon 3 of the murine *CIITA* gene was each cloned into the pX330 vector (carrying the Cas9 nuclease coding sequence; Addgene). The guide sequences (in uppercase) plus restriction overhangs (in lowercase) were as follows: *CIITA exon2* forward, 5'-caccGGGGGTCGGCATCACTGTTA-3' and reverse, 5'-aacTAACAGTGATGCCGACCC-3'; *CIITA exon3* forward, 5'-caccGCTGAACTGGTCGAGTTGA-3' and reverse, 5'-aacTCAACTGCGACCAGTTTCAGC-3'. To delete the target gene, lymphoma lines 775, 1019 and A20 were each transiently electroporated with pX330 vectors carrying sgRNAs that target *CIITA* exon 2 and exon 3. Three to six days after electroporation, MHC-II negative subsets of each line were purified by FACS sorting.

In vitro killing assay.

Target cells were labeled with CellTrace Violet (Invitrogen) before use. T cells were co-cultured with 2 × 10³ target cells at varying effector/target ratios for 4–6 h in 96-well round-

bottomed plates, followed by active Caspase-3 staining (BD Biosciences)^{6,29}. The blocking of mouse MHC-II and FasL was performed as described previously⁹. In human cell killing assays, target cells (CLL cells) were pre-incubated with HLA-II (HLA-DR, -DP, -DQ) blocking antibody (TÜ39) or isotype control mouse IgG2a (both at 2 µg/ml; BD Biosciences) for 20 min at 37°C. In all killing assays, effector/target mixtures in 96-well plates were spun down at 8 *g* for 2 min prior to the incubation at 37°C; cultures were stained for CD4 or CD8 (to exclude effector cells) and analyzed for active Caspase-3 levels in CellTrace-labeled target cells. Active Caspase-3⁺CellTrace⁺ cells represent apoptotic target cells. % specific killing = % apoptotic target cells in cultures with both effectors and targets - % apoptotic target cells in cultures with targets alone.

T cell proliferation assay for MHC restriction.

In one set of experiments, CD4 effector cells (excluding GFP⁺ Tregs) from the bone marrow of adult *Foxp3^{DTR/GFP};CL* male mice were sorted and stained with CellTrace, followed by a 6 h incubation in fresh RPMI media (to ensure that the T cells were at rest); the CD4 cells were then co-cultured with CD40-activated WT or *CIITA*^{-/-} B cell targets prepared as described above. In another set of experiments, CD4 cells primed *in vitro* by LMP1⁺ B cells were stained with CellTrace, and co-cultured with the following LMP1-negative lymphoma B cells: (1) line 773 in the presence of MHC-II (I-A/I-E) blocking antibody (M5/114.15.2) or isotype control rat IgG2b (both at 10 µg/ml; Biolegend) or (2) line 775 expressing or lacking *CIITA*. 1×10^5 CD4 cells were co-cultured with target cells (1×10^5 CD40-activated B cells or 0.2×10^5 lymphoma cells) for 3 days (on lymphoma cells) or 4 days (on CD40-activated B cells) in 96-well round-bottomed plate, followed by staining with anti-TCRβ, -CD4, -CD19 and Topro3, and FACS analysis of CellTrace dilution in the CD4 cells (Topro3⁻CellTrace^{low} populations represent live proliferating cells).

Gene expression profiling.

LMP1⁺ B cells and YFP control B cells were prepared as previously described⁹. CD40-activated B cells and control naive B cells (*ex vivo*) were prepared as described above. Subsequently, total RNA was extracted with TRIzol reagent (Invitrogen) according to manufacturer's instructions and analyzed on GeneChip Mouse Gene 2.0 ST arrays; the GeneChip data were scanned and analyzed by GeneChip Scanner 3000 7G with GeneChip Operating Software v1.3 (all Affymetrix) at the Molecular Biology Core Facility at DFCL.

Immunoblot analysis.

Mouse cells were lysed as described previously⁶. Protein extracts were fractionated on 8% (for LMP1 immunoblot), 10% (for Trp1 immunoblot) or 15% (for Survivin and EphA2 immunoblots) sodium dodecyl sulfate polyacrylamide gels, transferred onto polyvinylidene difluoride membranes and immunoblotted with the following primary antibodies: anti-LMP1 (clone S12, 1:4; obtained as described previously⁹), anti-Survivin (clone 71G4B7, 1:1000; Cell Signaling), anti-EphA2 (clone C-3, 1:200; Santa Cruz), anti-Trp1 (clone TA99, 1:100; Santa Cruz), anti-Flag (clone M2, 1:5000; Sigma) and anti-GAPDH (clone 2118, 1:1000; Cell Signaling). Images were taken with ImageQuant LAS 4000 using ImageQuant LAS 4000 v1.2 software (both GE Healthcare Life Sciences).

Tetramer staining.

PE- or APC-labeled H-2D^b tetramer loaded with Survivin_{20–28} (ATFKNWPFL)³⁰ or lymphocytic choriomeningitis virus glycoprotein (LCMV GP)_{33–41} (KAVYNFATC), and H-2K^b tetramer loaded with Ephrin type-A receptor 2 (EphA2)_{682–689} (VVSKYKPM)³¹ were obtained from the NIH tetramer facility. For tetramer staining, single-cell suspensions prepared from mouse spleens were first enriched for CD8⁺ cells via positive selection with anti-CD8 α microbeads (Miltenyi Biotec) and stained with a viability dye eFluor 506 for 30 min at 4°C. The cell suspensions were subsequently incubated with the tetramers for 30 min at room temperature in PBS containing 0.5% BSA, 1 mM EDTA and 0.05% NaN₃. After intensive washing, the cells were stained with anti-CD3 and -CD8 along with antibodies for a “dump channel” (FITC-conjugated anti-CD4, -CD11b, -CD19 and -CD49b; to exclude unwanted cell populations) for 20 min at 4°C, washed, and analyzed by FACS.

In vitro transcription and electroporation of mRNA.

cDNA for Trp1 (with a C-terminal Flag tag), LMP1 or GFP was each subcloned into the pcDNA3.1 vector (Addgene). The plasmids encoding Trp1, LMP1 or GFP (with an upstream T7 promoter) were linearized using XhoI (for pcDNA3.1-Trp1) or XbaI (for pcDNA3.1-LMP1 and -GFP), and subsequently transcribed *in vitro*, capped at 5' end and polyadenylated at 3' end using an mMESSAGE mMACHINE T7 Ultra Kit (Life Technologies) per the supplier's protocol. Electroporation of the mRNAs was done using Amaxa 4D-Nucleofector device (Lonza) under the program DI-100 (for 1019 cells) or EO-117 (for CLL cells); for 1019 cells, 15 μ g of Trp1 mRNA was electroporated in 100 μ l Amaxa P4 solution; for CLL cells, 15 μ g of GFP or LMP1 mRNA was electroporated in 100 μ l Amaxa P3 solution. One to two days after electroporation, cells were analyzed by FACS or used in subsequent experiments.

In vitro T cell stimulation.

Mouse T cells were enriched from splenocytes by negative selection with an antibody cocktail (anti-CD11b, -CD19, -B220, -Gr-1 and -Ter119) using MACS (StemCell Technologies), and then FACS-sorted for naive CD4 cells—CD4⁺CD44^{low}CD62L^{high}CD25⁻, except for those from Trp1 mice which were CD4⁺CD25⁻CD69⁻. Subsequently, purified naive CD4 cells were primed *in vitro* as follows: (1) Trp1-specific CD4 CTLs: the CD4 cells from Trp1 mice were plated in 96-well round-bottomed plates at 1.2×10^5 per well with irradiated (5 Gy) Trp1-transfected 1019 cells (LMP1-driven B cell line) at a 2:1 ratio. The CD4 cells were re-stimulated at day 5 with the target cells under the same conditions for an additional 3 days; (2) CD4 CTLs by LMP1⁺ B cells: the CD4 cells from WT B6 mice were plated in 24-well plates at 1×10^6 per well with irradiated (5 Gy) LMP1⁺ B cells at a 2:1 ratio. Five days later, the CD4 cells were re-stimulated with the same targets under identical conditions for another 2–3 days; (3) CD4 CTLs by LMP1-A20 cells: the CD4 cells from WT BALB/c or CD45.1⁺ congenic mice were cultured in 24-well plates at 1×10^6 per well with irradiated (5 Gy) LMP1-expressing A20 cells at a 2:1 ratio for 6–7 days (without re-stimulation); and (4) Th0 cells: the CD4 cells from CD45.1⁺ congenic BALB/c mice, 2×10^5 per well in 24-well plates, were stimulated for 3 days with plate-bound anti-CD3 (clone 145–2C11, 2 μ g/ml; Biolegend) and soluble anti-CD28 (clone

37.51, 1 µg/ml; eBioscience), with addition of recombinant human IL-2 (30 IU/ml; NCI Biological Resource Branch) from day 2 onwards. After the indicated periods of *in vitro* culture, the primed CD4 cells were harvested for FACS analysis or sorted for adoptive transfer experiments. All cells were cultured in RPMI 1640 medium supplemented with 10% FBS, 100 IU/ml penicillin, 10 mM HEPES, 1× non-essential amino acids, 1 mM sodium pyruvate (Gibco) and 50 µM β-mercaptoethanol, without addition of any growth factors or cytokines except where indicated.

For stimulation of autologous CD4 cells on LMP1-expressing CLL cells, patient CD4⁺CD25^{low/-} T cells were isolated as described above. The CD4 cells were plated with irradiated (5 Gy) LMP1-transfected CLL cells at a 2:1 ratio. Four to seven days later, the CD4 cells were re-stimulated with the targets under the same conditions for another 4–6 days. All human cells were cultured in RPMI 1640 medium supplemented with 10% AB-positive human serum, 100 IU/ml penicillin, 10 mM HEPES, 1× non-essential amino acids, 1 mM sodium pyruvate and 50 µM β-mercaptoethanol, without addition of any growth factors or cytokines. HLA-II-restricted killing of the stimulated CD4 cells was tested in the same medium but containing 10% FBS instead of human serum to exclude potential CD4 responses against any serum antigens.

Activation-induced marker assays.

Mouse Trp1-specific naive CD4 cells (purified as described above) were stimulated with target cells at a 1:1 ratio for 18 h in 96-well round-bottomed plates at 37°C and 5% CO₂ in an incubator. The cultures were then stained for CD69, CD4 and CD19, and analyzed for CD69 levels in the CD4 cells to indicate their activation. In the set of experiments to assess Trp1 presentation by MHC-II via endogenous versus exogenous pathway, the 1019 variants (MHC-II⁺ or MHC-II⁻) were transfected with or without Trp1 mRNA, and then mixed at 1:1 right after transfection as indicated, and 1 day later co-cultured with naive Trp1-specific CD4 cells for CD69 upregulation assay. For human cells, CD69/CD40L upregulation was used to indicate CD4 cell activation. Effector/memory CD4 cells from CLL patients were isolated as described above, and the assays were performed as described previously³² except that CD4 cells were incubated with targets at a 1:1 ratio for 18 h. The cells were subsequently stained for CD69, CD40L, CD4 and CD19, and analyzed for the levels of CD69 and CD40L in the CD4 cells.

Tumour model, adoptive T cell transfer and PD-1 blockade.

A20 lymphoma B cells were injected subcutaneously (S.C.; 3×10^5 per mouse) into the left flank of syngeneic female BALB/c mice (6–8 weeks of age). At day 7 after tumour implantation, mice bearing tumours of similar sizes were randomly assigned to treatment with 6 Gy of total body irradiation (TBI), and 4–6 h later with infusion of CD4 CTLs primed by LMP1-A20 cells or naive CD4 cells as control (0.4×10^6 each; both containing ~6% CD4⁺ Tregs). For PD-1 blockade, animals treated with or without the CD4 CTLs as described above were injected intraperitoneally (I.P.; 100 µg per mouse) with PD-1 blocking antibody (clone 29F.1A12) or isotype control antibody (clone 2A3) (both from BioXCell) at days 15 and 19 post-tumour challenge. Tumours were measured unblinded with a caliper every two days, and the tumour volume was calculated using the following formula: ($A \times$

$B^2)/2$ (A as the largest and B the smallest diameter of the tumour). Animals were euthanized when their tumours reached 20 mm in any direction or when they exhibited signs of impaired health.

T cell isolation from A20 tumours.

To distinguish adoptively transferred CD4 cells from endogenous CD4 cells in the A20 tumour-grafted mice (CD45.2⁺), naive CD4 cells were prepared from CD45.1⁺ congenic mice and differentiated into the desired CD4 cell lineages. The CD4 cells were transferred intravenously (I.V.) into A20-bearing mice as described above. At day 8 after T cell transfer, A20 tumours were harvested and minced into pieces of 1–2 mm diameter, then digested for 1 h in RPMI supplemented with 2% FBS, 20 U/ml DNase I (Roche) and 50 U/ml collagenase type IV (Roche) at 37°C. The resultant cell suspensions were washed twice with RPMI supplemented with 2% FBS and passed through a 70- μ m cell strainer, followed by FACS analysis of intra-tumoural T cells.

Interferon (IFN)- γ enzyme-linked immunospot (ELISPOT).

To identify TAAs involved in the CD4 cell recognition of CLL cells, autologous CD4 cells were stimulated by LMP1-expressing CLL cells as described above; in the cases (Patients 7 and 10) where insufficient numbers of CD4 cells were obtained by this initial expansion, the CD4 cells were additionally stimulated for 15 days with the same targets in the presence of recombinant human IL-7 (20 ng/ml; Biolegend), with addition of low-dose recombinant human IL-2 (20 IU/ml) from day 3 onwards. The expanded CD4 cells were rested overnight in cytokine-free medium before plating for ELISPOT assay. When unstimulated (*ex vivo*) CD4 cells were tested in the assay, they were used without prior resting. ELISPOT assays were conducted using 96-well MultiScreen Filter Plates (Millipore), coated with 2 μ g/ml anti-IFN- γ (clone 1-D1K; Mabtech) overnight. Plates were rinsed with PBS and blocked for 2 h with RPMI 1640 medium containing 10% FBS and 100 IU/ml penicillin (complete medium). CD4 cells ($0.5\text{--}2 \times 10^4$ cells per well) were co-cultured for 24 h with antigen-presenting cells (APCs; described below) at a 2:1 or 4:1 ratio in the presence of the following individual (10 μ g/ml) or pooled peptides (5 μ g/ml each) (all from GenScript): CTSH_{185–198} (LPSQAFEYILYNKG), TFRC_{198–210} (NSVIIVDKNGRLV) plus TFRC_{680–693} (RVEYHFLSPYVSPK), VAMP2_{44–60} (DIMRVNVDKVLERDQKL) plus VAMP2_{50–66} (VDKVLERDQKLSELDDR) or HIV p24_{164–181} (YVDRFYKTLRAEQASQEV; negative control). CD4 cells treated with 0.1 μ M PMA and 1 μ M ionomycin served as positive control. Subsequently, plates were incubated with 1 μ g/ml biotinylated anti-IFN- γ (clone 7-B6–1; Mabtech) and then Streptavidin-Alkaline Phosphatase (ALP) (Mabtech), followed by SIGMA FAST BCIP/NBT (5-bromo-4-chloro-3-indolyl phosphate/nitro blue tetrazolium) substrate to develop the immunospots. Spots were imaged and analyzed by an ImmunoSpot S6 Micro Analyzer with ImmunoSpot 5.1.36 software (both Cellular Technology Limited). In some experiments, to block peptide presentation, APCs were pre-incubated with 5 μ g/ml HLA-II blocking antibodies (clone TÛ39) for 1 h before the addition of CD4 cells and peptides to the wells. A response was scored positive when at least 10 spot-forming cells (SFC) per 10^4 CD4 cells were detected and the mean spot count per well was > 3-fold higher than the mean number of spots in the negative control wells. Dendritic cells (DCs) as APCs were generated from autologous

CD14⁺ monocytes by culturing with recombinant human GM-CSF (120 ng/ml) and recombinant human IL-4 (70 ng/ml) (both from Biolegend) in complete medium. On day 6, 30 µg/ml polyinosinic:polycytidylic acid (polyI:C; Sigma) was added to the culture to induce DC maturation, and 1–2 days later the cells were used as APCs.

Determination of EBV infection status.

To determine whether the CLL patients involved in the CD4 cell studies were previously infected with EBV, their plasma samples were tested for circulating IgG class antibodies against EBV viral capsid antigen (VCA) with enzyme-linked immunosorbent assay (ELISA) kit (Gold Standard Diagnostics). The assays were carried out according to the manufacturer's instructions; data were scored, based on their index value, as positive (≥ 1.1), negative (< 0.9) or equivocal (0.9–1.09).

Histology.

Mouse tissues were fixed with 10% formalin (Sigma), embedded in paraffin and sectioned at 5 µm. The sections were subsequently stained with hematoxylin and eosin (H&E), and examined microscopically.

Statistical Analysis.

Data analyses were performed using Prism v7.03 (GraphPad). Statistical significance was determined by unpaired two-tailed Student's *t* test, except where indicated otherwise; a *P* value < 0.05 was considered significant (**P* < 0.05 , ***P* < 0.01 , ****P* < 0.001 and *****P* < 0.0001). Survival curves were compared using log-rank (Mantel-Cox) test.

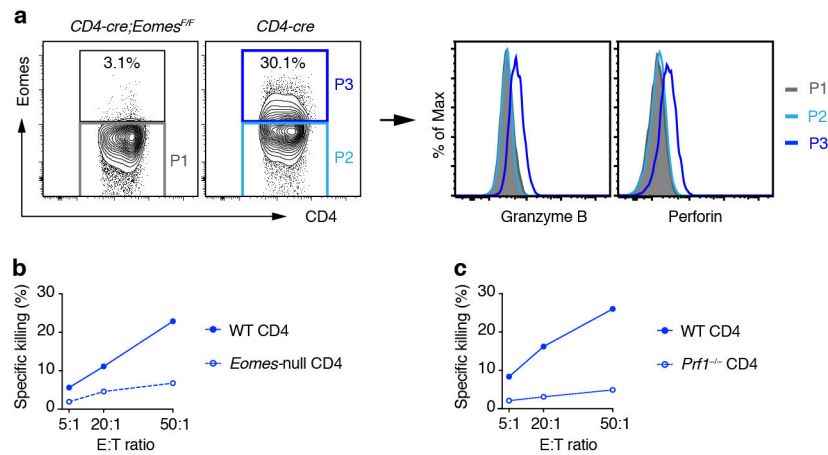
Data availability.

The microarray data have been deposited to the NCBI GEO (accession number GSE159854). All other data from the manuscript are available from the corresponding author upon reasonable request. Source data are provided with this paper.

Code availability.

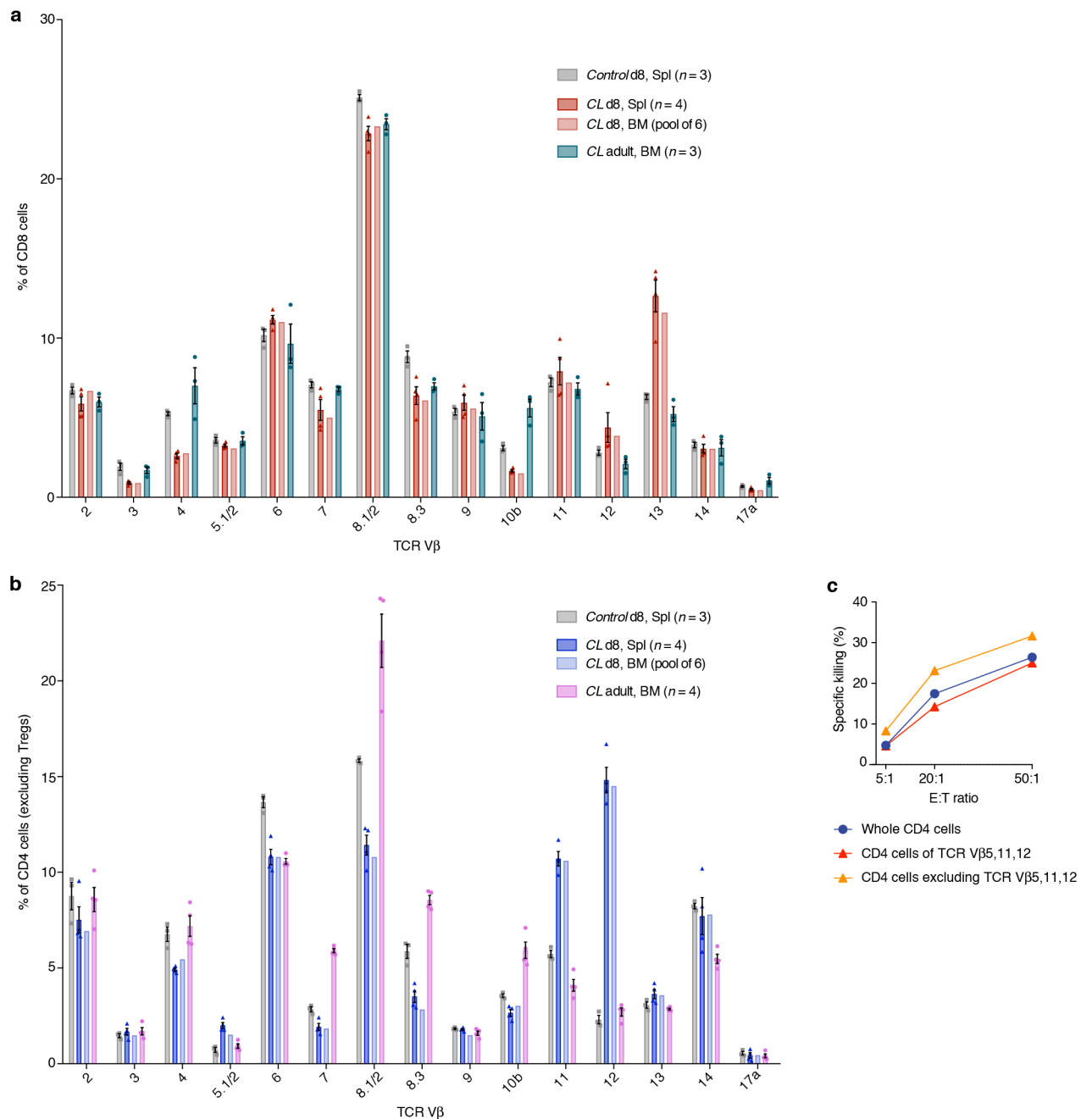
No custom code or mathematical algorithm was used in this work.

Extended Data

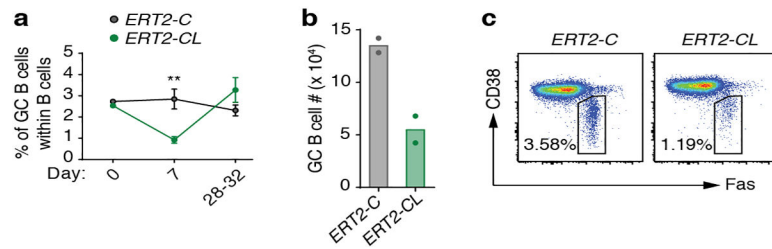


Extended Data Fig. 1. LMP1⁺ B cells drive CD4⁺ T cell differentiation into Eomes-programmed granzyme/perforin-dependent cytotoxic effectors.

a, FACS analysis of Eomes, Granzyme B and Perforin expression in CD4 cells, from mice with CD4-specific Eomes knockout (*CD4-cre;Eomes^{F/F}*) or with normal levels of Eomes (*CD4-cre*), primed *in vitro* by LMP1⁺ B cells. Granzyme B and Perforin levels in Eomes⁺ CD4 cells from *CD4-cre* mice (P3) were compared with those in Eomes⁻ CD4 cells from the same mice (P2) or *CD4-cre;Eomes^{F/F}* mice (P1), and are shown on the right. For these analyses, Foxp3⁺ Tregs were excluded. **b**, **c**, Killing activity of Eomes-null CD4 cells (from *CD4-cre;Eomes^{F/F}* mice) or perforin-null CD4 cells (from *Prf1^{-/-}* mice) in comparison with WT CD4 cells, primed as in **a**, against LMP1⁺ lymphoma cell targets. E:T ratio, effector-to-target cell ratio. All mice are on the B6 background. Statistics and reproducibility are in Supplementary Information.

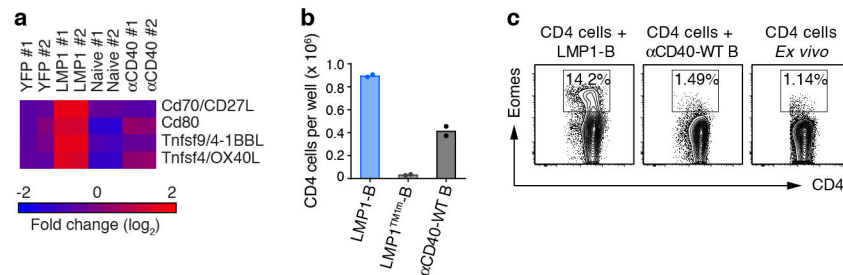


Extended Data Fig. 2. CD4 and CD8 cells mount a polyclonal response to LMP1⁺ B cells.
a, b, Analysis of TCR V β repertoire on CD8 cells (**a**) and CD4 cells (excluding Foxp3⁺ Tregs) (**b**) from spleen (Spl) or bone marrow (BM) of control or *CL* mice, using a panel of monoclonal antibodies for the indicated V β chains. These antibodies collectively detected 85–95% of TCRs in all the samples. The majority of CD4 and CD8 cells in the spleen and BM of 8-day-old *CL* mice and BM of adult *CL* mice were CD44⁺CD62L⁻ effector/memory cells^{6,9}. *Control* d8, 8-day-old *CD19-cre*^{+/+} mice; *CL* adult, 6–12-week-old *CL* mice. In **a–b**, data are shown as mean \pm s.e.m. **c,** *In vitro* killing of LMP1⁺ lymphoma cells by the indicated CD4 subsets from 6–8-day-old *CL* mice. All mice are on the CB6F1 background.



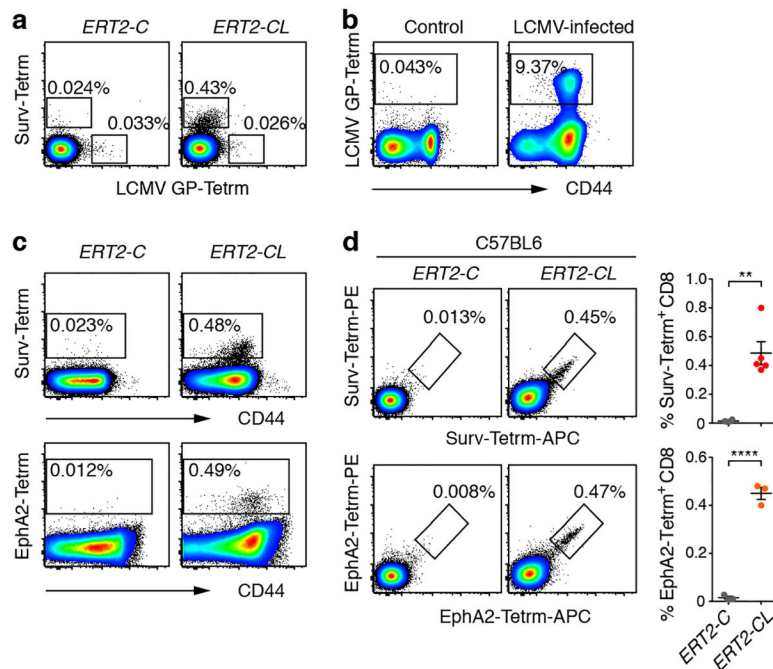
Extended Data Fig. 3. Transient reduction of germinal center (GC) B cells around the time of peak T cell response.

a, Frequency of spontaneous GC B cells ($CD19^+Fas^{high}CD38^{low}$) analyzed by FACS in the mesenteric lymph nodes of the inducible LMP1-expressing *ERT2-CL* mice and littermate controls (*ERT2-C*) after tamoxifen treatment. Error bars denote mean \pm s.e.m. **b, c**, Numbers (**b**) and representative FACS plots (**c**) of GC B cells from the indicated mice 7 days post-tamoxifen treatment as in **a**.

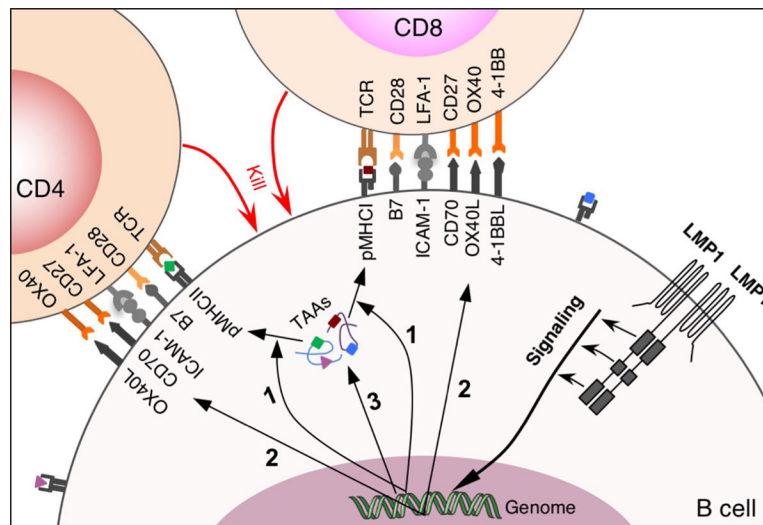


Extended Data Fig. 4. LMP1 signaling and CD40 activation in B cells lead to differential expression of costimulatory ligands.

a, Relative transcript levels of the indicated costimulatory molecules in $LMP1^+$ B cells compared with CD40-activated B cells and control B cells. Splenic B cells from *LMP1^{flSTOP}/YFP^{flSTOP}* and *YFP^{flSTOP}/+* mice (both on the CB6F1 background) were treated with TAT-Cre to generate $LMP1^+$ B cells and YFP control B cells; naive B cells (*ex vivo*) and α CD40-activated B cells were prepared from B6 mice. All treated B cells were analyzed 2 days post-treatment. **b**, Numbers (mean) of CD4 cells recovered after 7-day co-culture with B cells expressing LMP1 or the signaling dead mutant $LMP1^{TM1m}$, or pre-activated with anti-CD40 antibody. Purified CD4 cells (1.5×10^6) were cultured with irradiated B cells as indicated at 1:1 ratio in duplicate wells of 12-well plates. No exogenous cytokine was added. **c**, Eomes expression in CD4 cells co-cultured with the indicated B cells as in **b**. *Ex vivo* CD4 cells served as control. B and T cells in **b-c** are from spleens of 2–3-month-old naive B6 mice.

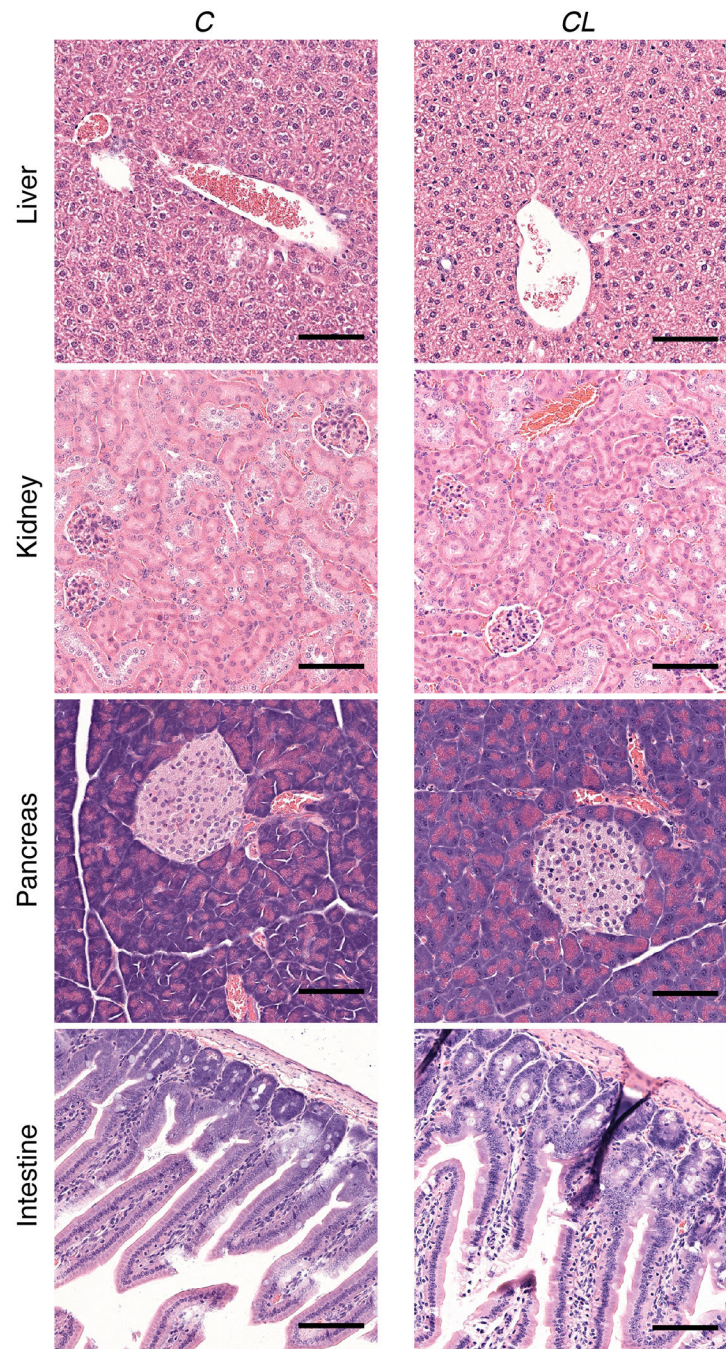


Extended Data Fig. 5. Specificity analysis of CD8 cells in *ERT2-CL* mice using MHC-I tetramers.
a, Representative FACS analysis of splenic CD8 cells from control mice (*ERT2-C*) or mice expressing inducible LMP1 (*ERT2-CL*) stained with Survivin_{20–28} tetramer (Surv-Tetrm) versus an irrelevant control tetramer (H-2D^b loaded with the LCMV GP_{33–41} epitope peptide (LCMV GP-Tetrm)). **b**, Validation of the LCMV GP-tetramer by staining splenic CD8 cells from LCMV (clone 13)-infected mice at day 8 post-infection, versus uninfected control mice. **c**, Representative FACS analysis of splenic CD8 cells from the indicated mice stained with anti-CD44 and Surv-Tetrm (upper) or EphA2_{682–689} tetramer (EphA2-Tetrm) (lower). **d**, FACS analysis of splenic CD8 cells from the indicated mice stained with the indicated tetramers labeled with PE and APC. Representative FACS plots are shown on the left, and summary data on the right. Each circle represents one mouse; bars show mean \pm s.e.m. All *ERT2-CL* and littermate control mice were analyzed on day 5 after tamoxifen treatment. Mice used in **a**, **c** are on the CB6F1 background; in **b**, **d** on the B6 background.



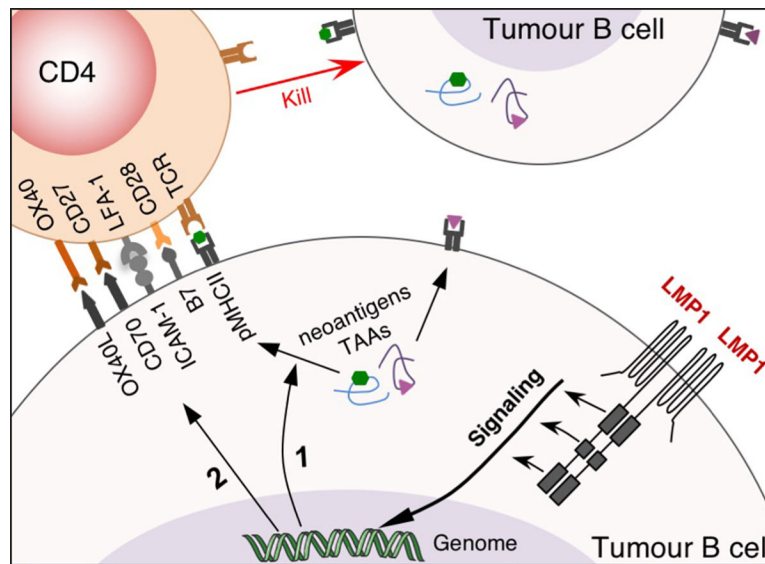
Extended Data Fig. 6. Schematic view of how LMP1 signaling in B cells induces cytotoxic CD4 and CD8 T cell responses to TAAs.

LMP1 signaling in B cells induces massive cellular gene expression. This leads to (1) upregulation of cellular machinery involved in antigen processing and presentation, (2) upregulation of costimulatory ligands (CD70, OX40L and others), and (3) overexpression of many cellular antigens known as TAAs. Presentation of the LMP1-induced cellular antigens/TAAs and simultaneous costimulation through CD70 and OX40L drive cytotoxic CD4 and CD8 T cell responses.

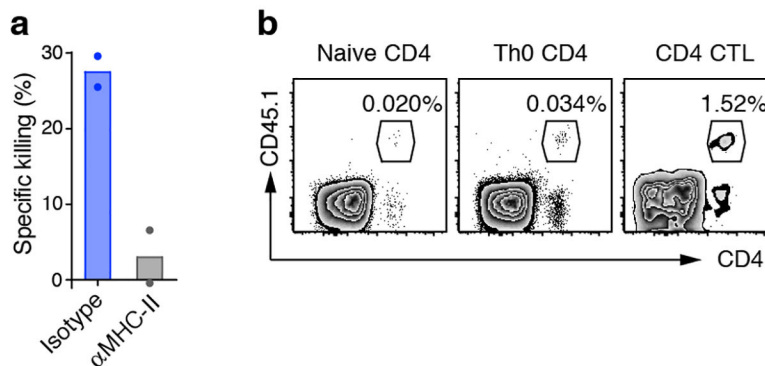


Extended Data Fig. 7. No discernible pathological changes in non-lymphoid tissues of LMP1 mice after contraction of the T cell response.

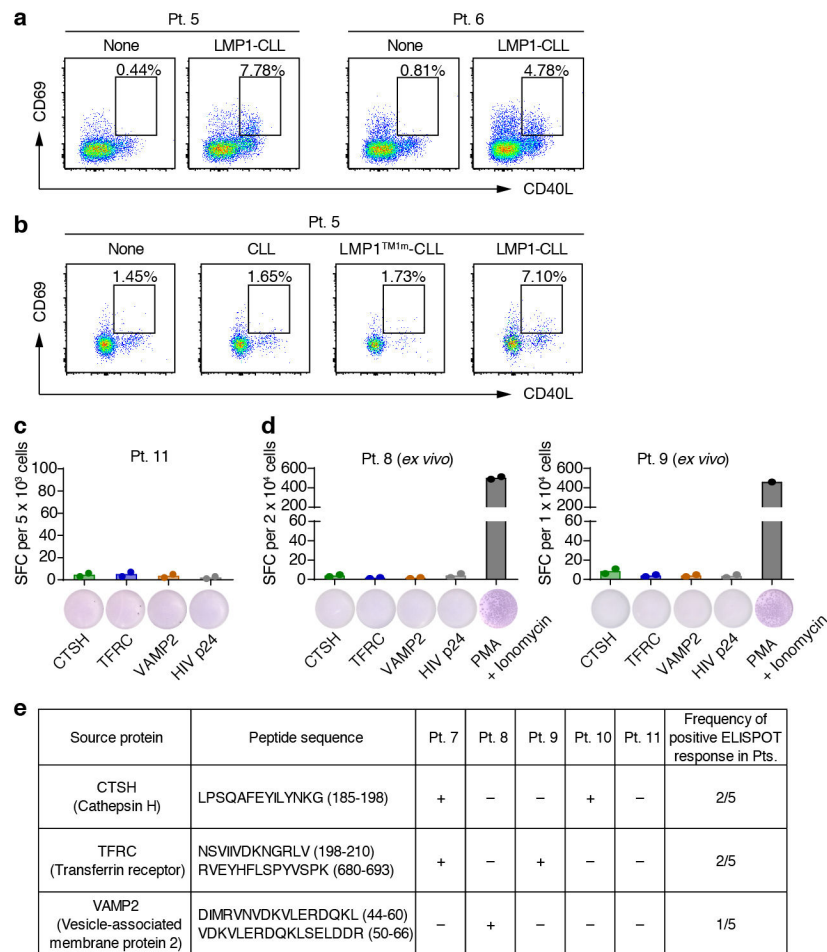
Representative hematoxylin and eosin (H&E) staining of liver, kidney, pancreas and intestine sections from control (*C*) and *CL* mice at 6–7 weeks after birth, at which time the T cell response against LMP1⁺ B cells has contracted⁹. All mice are on the CB6F1 background. Scale bar, 1000 μ m.



Extended Data Fig. 8. Schematic of the proposed LMP1-based CD4 CTL therapeutic strategy. Ectopically expressing LMP1 in patient tumour B cells will (1) enhance presentation of endogenous antigens, such as TAAs and neoantigens, on MHC-II, and (2) provide costimulation through CD70 and OX40L, thereby eliciting CD4 CTLs against these tumour antigens. CD4 CTLs generated in this fashion will mediate cytotoxicity to unmodified tumour B cells that express the same antigens.



Extended Data Fig. 9. Characterization of CD4 CTLs primed by LMP1-transduced A20 cells. **a**, Cytotoxicity of CD4 CTLs primed by LMP1-A20 cells against the B-cell lymphoma line BCL1 at an E:T ratio of 50:1, in the presence of MHC-II blocking antibody or isotype control antibody. **b**, Representative FACS analysis of intra-tumoural CD45.1⁺ adoptive CD4 cells (excluding Foxp3⁺) recovered from A20-bearing mice (CD45.2⁺) treated as in Fig. 3g–i. All mice are on the BALB/c background.



Extended Data Fig. 10. Reactivity analysis of autologous CD4 cells before and after stimulation with LMP1-transfected patient tumour B cells.

a, Co-expression of CD69 and CD40L in effector/memory CD4 cells from two CLL patients after culturing 18 h with or without LMP1-transfected CLL cells (LMP1-CLL). Pt., patient. **b**, Co-expression of CD69 and CD40L in effector/memory CD4 cells from a CLL patient assessed after culturing 18 h alone, with untransfected CLL cells, LMP1^{TM1m}- or LMP1-transfected CLL cells. **c**, **d**, Analysis of IFN- γ ELISPOT responses of CD4 cells pre-stimulated with LMP1-CLL (**c**) or unstimulated (*ex vivo*) CD4 cells (**d**), against individual (CTSH₁₈₅₋₁₉₈) or pooled (TFRC₁₉₈₋₂₁₀ plus TFRC₆₈₀₋₆₉₃ or VAMP2₄₄₋₆₀ plus VAMP2₅₀₋₆₆) epitope peptides from the selected CLL TAAs pulsed on autologous dendritic cells. PMA- and ionomycin-stimulated CD4 cells served as positive control; an irrelevant HIV p24₁₆₄₋₁₈₁ peptide as negative control. Numbers of spot-forming cells (SFC) in individual wells and their mean value per initial seeding number of CD4 cells are presented on the y-axis; representative ELISPOT images below the x-axis. **e**, Summary of IFN- γ ELISPOT responses of the CD4 cells pre-stimulated with LMP1-CLL, against the indicated CLL TAA epitopes in the five CLL patients tested (Pt. 11 in **c**; Pts. 7, 8, 9 and 10 in Fig. 4f). +, positive ELISPOT response (see Methods); -, no response.

Supplementary Material

Refer to Web version on PubMed Central for supplementary material.

Acknowledgments:

We thank the DFCI HN Flow Cytometry Core for assistance with the flow cytometry studies and cell sorting, the Pasquarello Tissue Bank in Hematologic Malignancies and the CLL Center Tissue Bank for patient samples, and the Dana-Farber/Harvard Cancer Center (DF/HCC) Specialized Histopathology Core for providing histology service. DF/HCC is supported in part by an NCI Cancer Center Support Grant (NIH 5P30CA06516). We thank D.P. Leahy and B. Beaulieu for administrative assistance and P. McCaffrey for valuable input. We are grateful to the NIH Tetramer Facility at Emory University for providing the tetramers. This work was supported in part by DFCI Faculty Startup Funds, Medical Oncology Translational Grant, and Claudia Adams Barr Award to B.Z.; the American Cancer Society Research Scholar Grant RSG-19-035-01-LIB to B.Z.; the Leukemia & Lymphoma Society grant TRP-6595-20 to B.Z.; the Wade F.B. Thompson/Cancer Research Institute CLIP Grant to B.Z.; the Claudia Adams Barr Program for Innovative Cancer Research to I.K.C.; NIH grant P01CA206978-01 to J.R.B.

References

1. Coulie PG, Van den Eynde BJ, van der Bruggen P & Boon T Tumour antigens recognized by T lymphocytes: at the core of cancer immunotherapy. *Nature reviews. Cancer* 14, 135–146, doi:10.1038/nrc3670 (2014). [PubMed: 24457417]
2. Blankenstein T, Coulie PG, Gilboa E & Jaffee EM The determinants of tumour immunogenicity. *Nature reviews. Cancer* 12, 307–313, doi:10.1038/nrc3246 (2012). [PubMed: 22378190]
3. Long HM et al. CD4+ T-cell clones recognizing human lymphoma-associated antigens: generation by in vitro stimulation with autologous Epstein-Barr virus-transformed B cells. *Blood* 114, 807–815, doi:10.1182/blood-2008-12-194043 (2009). [PubMed: 19443664]
4. Iheagwara UK et al. Influenza virus infection elicits protective antibodies and T cells specific for host cell antigens also expressed as tumor-associated antigens: a new view of cancer immunosurveillance. *Cancer immunology research* 2, 263–273, doi:10.1158/2326-6066.CIR-13-0125 (2014). [PubMed: 24778322]
5. Taylor GS, Long HM, Brooks JM, Rickinson AB & Hislop AD The immunology of Epstein-Barr virus-induced disease. *Annual review of immunology* 33, 787–821, doi:10.1146/annurev-immunol-032414-112326 (2015).
6. Zhang B et al. Immune surveillance and therapy of lymphomas driven by Epstein-Barr virus protein LMP1 in a mouse model. *Cell* 148, 739–751, doi:10.1016/j.cell.2011.12.031 (2012). [PubMed: 22341446]
7. Yasuda T et al. Studying Epstein-Barr Virus Pathologies and Immune Surveillance by Reconstructing EBV Infection in Mice. *Cold Spring Harbor symposia on quantitative biology*, doi:10.1101/sqb.2013.78.020222 (2013).
8. Pearce EL et al. Control of effector CD8+ T cell function by the transcription factor Eomesodermin. *Science* 302, 1041–1043, doi:10.1126/science.1090148 (2003). [PubMed: 14605368]
9. Choi IK et al. Signaling by the Epstein-Barr virus LMP1 protein induces potent cytotoxic CD4(+) and CD8(+) T cell responses. *Proceedings of the National Academy of Sciences of the United States of America* 115, E686–E695, doi:10.1073/pnas.1713607115 (2018). [PubMed: 29311309]
10. Smith C et al. Discerning regulation of cis- and trans-presentation of CD8+ T-cell epitopes by EBV-encoded oncogene LMP-1 through self-aggregation. *Blood* 113, 6148–6152, doi:10.1182/blood-2009-02-203687 (2009). [PubMed: 19372256]
11. Acha-Orbea H & MacDonald HR Superantigens of mouse mammary tumor virus. *Annual review of immunology* 13, 459–486, doi:10.1146/annurev.iy.13.040195.002331 (1995).
12. Thorley-Lawson DA Epstein-Barr virus: exploiting the immune system. *Nature reviews. Immunology* 1, 75–82, doi:10.1038/35095584 (2001).
13. Schultze JL et al. Follicular lymphomas can be induced to present alloantigen efficiently: a conceptual model to improve their tumor immunogenicity. *Proceedings of the National Academy of Sciences of the United States of America* 92, 8200–8204 (1995). [PubMed: 7545296]

14. Kaye KM, Izumi KM & Kieff E Epstein-Barr virus latent membrane protein 1 is essential for B-lymphocyte growth transformation. *Proceedings of the National Academy of Sciences of the United States of America* 90, 9150–9154 (1993). [PubMed: 8415670]
15. Muranski P et al. Tumor-specific Th17-polarized cells eradicate large established melanoma. *Blood* 112, 362–373, doi:10.1182/blood-2007-11-120998 (2008). [PubMed: 18354038]
16. Brooks A et al. Class II-restricted presentation of an endogenously derived immunodominant T-cell determinant of hen egg lysozyme. *Proceedings of the National Academy of Sciences of the United States of America* 88, 3290–3294, doi:10.1073/pnas.88.8.3290 (1991). [PubMed: 1707537]
17. Dengjel J et al. Autophagy promotes MHC class II presentation of peptides from intracellular source proteins. *Proceedings of the National Academy of Sciences of the United States of America* 102, 7922–7927, doi:10.1073/pnas.0501190102 (2005). [PubMed: 15894616]
18. Paludan C et al. Endogenous MHC class II processing of a viral nuclear antigen after autophagy. *Science* 307, 593–596, doi:10.1126/science.1104904 (2005). [PubMed: 15591165]
19. Challa-Malladi M et al. Combined genetic inactivation of beta2-Microglobulin and CD58 reveals frequent escape from immune recognition in diffuse large B cell lymphoma. *Cancer cell* 20, 728–740, doi:10.1016/j.ccr.2011.11.006 (2011). [PubMed: 22137796]
20. Roemer MGM et al. Major Histocompatibility Complex Class II and Programmed Death Ligand 1 Expression Predict Outcome After Programmed Death 1 Blockade in Classic Hodgkin Lymphoma. *Journal of clinical oncology : official journal of the American Society of Clinical Oncology* 36, 942–950, doi:10.1200/JCO.2017.77.3994 (2018). [PubMed: 29394125]
21. Elpek KG, Lacelle C, Singh NP, Yolcu ES & Shirwan H CD4+CD25+ T regulatory cells dominate multiple immune evasion mechanisms in early but not late phases of tumor development in a B cell lymphoma model. *Journal of immunology* 178, 6840–6848, doi:10.4049/jimmunol.178.11.6840 (2007).
22. Kowalewski DJ et al. HLA ligandome analysis identifies the underlying specificities of spontaneous antileukemia immune responses in chronic lymphocytic leukemia (CLL). *Proceedings of the National Academy of Sciences of the United States of America* 112, E166–175, doi:10.1073/pnas.1416389112 (2015). [PubMed: 25548167]
23. Bollard CM et al. Sustained complete responses in patients with lymphoma receiving autologous cytotoxic T lymphocytes targeting Epstein-Barr virus latent membrane proteins. *Journal of clinical oncology : official journal of the American Society of Clinical Oncology* 32, 798–808, doi:10.1200/JCO.2013.51.5304 (2014). [PubMed: 24344220]
24. Jayasooriya S et al. Early virological and immunological events in asymptomatic Epstein-Barr virus infection in African children. *PLoS pathogens* 11, e1004746, doi:10.1371/journal.ppat.1004746 (2015). [PubMed: 25816224]
25. Dunmire SK, Grimm JM, Schmeling DO, Balfour HH Jr. & Hogquist KA The Incubation Period of Primary Epstein-Barr Virus Infection: Viral Dynamics and Immunologic Events. *PLoS pathogens* 11, e1005286, doi:10.1371/journal.ppat.1005286 (2015). [PubMed: 26624012]
26. Haabeth OA et al. How Do CD4(+) T Cells Detect and Eliminate Tumor Cells That Either Lack or Express MHC Class II Molecules? *Frontiers in immunology* 5, 174, doi:10.3389/fimmu.2014.00174 (2014). [PubMed: 24782871]

Methods references

27. Zhang B et al. An oncogenic role for alternative NF-kappaB signaling in DLBCL revealed upon deregulated BCL6 expression. *Cell Rep* 11, 715–726, doi:10.1016/j.celrep.2015.03.059 (2015). [PubMed: 25921526]
28. Koralov SB et al. Dicer ablation affects antibody diversity and cell survival in the B lymphocyte lineage. *Cell* 132, 860–874, doi:10.1016/j.cell.2008.02.020 (2008). [PubMed: 18329371]
29. He L et al. A sensitive flow cytometry-based cytotoxic T-lymphocyte assay through detection of cleaved caspase 3 in target cells. *J Immunol Methods* 304, 43–59, doi:10.1016/j.jim.2005.06.005 (2005). [PubMed: 16076473]

30. Cui Y et al. Thymic expression of a T-cell receptor targeting a tumor-associated antigen coexpressed in the thymus induces T-ALL. *Blood* 125, 2958–2967, doi:10.1182/blood-2014-10-609271 (2015). [PubMed: 25814528]
31. Yamaguchi S et al. Immunotherapy of murine colon cancer using receptor tyrosine kinase EphA2-derived peptide-pulsed dendritic cell vaccines. *Cancer* 110, 1469–1477, doi:10.1002/cncr.22958 (2007). [PubMed: 17685394]
32. Porichis F et al. Differential impact of PD-1 and/or interleukin-10 blockade on HIV-1-specific CD4 T cell and antigen-presenting cell functions. *Journal of virology* 88, 2508–2518, doi:10.1128/JVI.02034-13 (2014). [PubMed: 24352453]

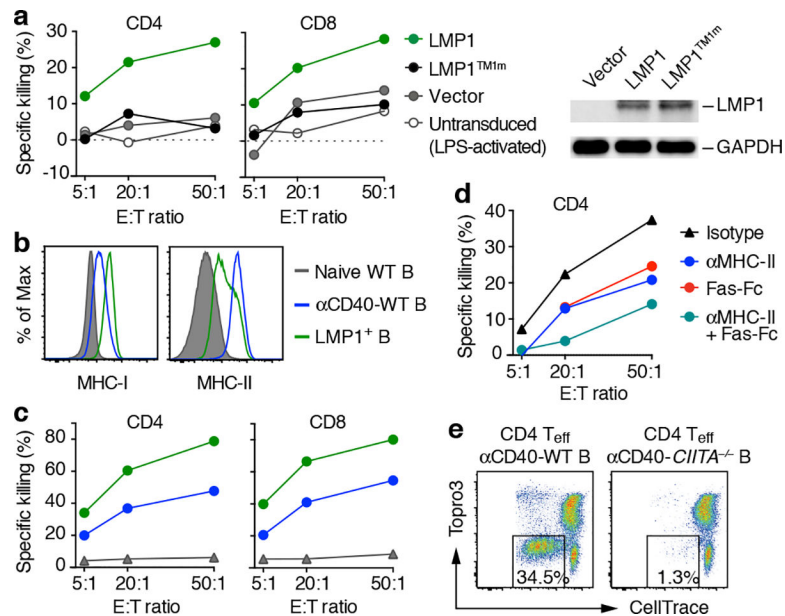


Fig. 1. T cells from *CL* mice recognize CD40-activated B cells lacking LMP1.

a, Left panel, *in vitro* cytotoxicity of CD4⁺ and CD8⁺ T cells from 6–8-day-old *CL* mice against B cells transduced to express LMP1 or its signaling-dead mutant (LMP1^{TM1m})⁹. B cells transduced with an empty vector or untransduced LPS-activated B cells (see Methods) served as controls. E:T ratio, effector-to-target cell ratio. Right panel, immunoblot of LMP1 and the mutant in the transduced B cells, with GAPDH as loading control. **b**, FACS analysis of MHC-I and -II levels on LMP1⁺ B cells and anti-CD40-activated WT B cells, compared to naive WT B cells. LMP1⁺ B cells were prepared by treating B cells from *LMP1^{flSTOP}* mice with TAT-Cre *in vitro*. **c**, Cytotoxicity of CD4 and CD8 cells from 6–8-day-old *CL* mice against naive, α CD40-activated or LMP1⁺ B cells prepared as in **b**. **d**, Cytotoxicity of CD4 cells from 6–8-day-old *CL* mice against CD40-activated B cells, in the presence of Fas-Fc (to block FasL) and/or MHC-II blocking antibody, or isotype control antibodies. **e**, Proliferation of CD4 effector cells from *Foxp3^{DTR/GFP}*; *CL* mice, co-cultured with CD40-activated B cells from WT or MHC-II–null *CIITA^{-/-}* mice. All *CL* mice are on the CB6F1 background, and all B cells on B6 background except those in **b** and **c** (CB6F1). Statistics and reproducibility are in Supplementary Information.

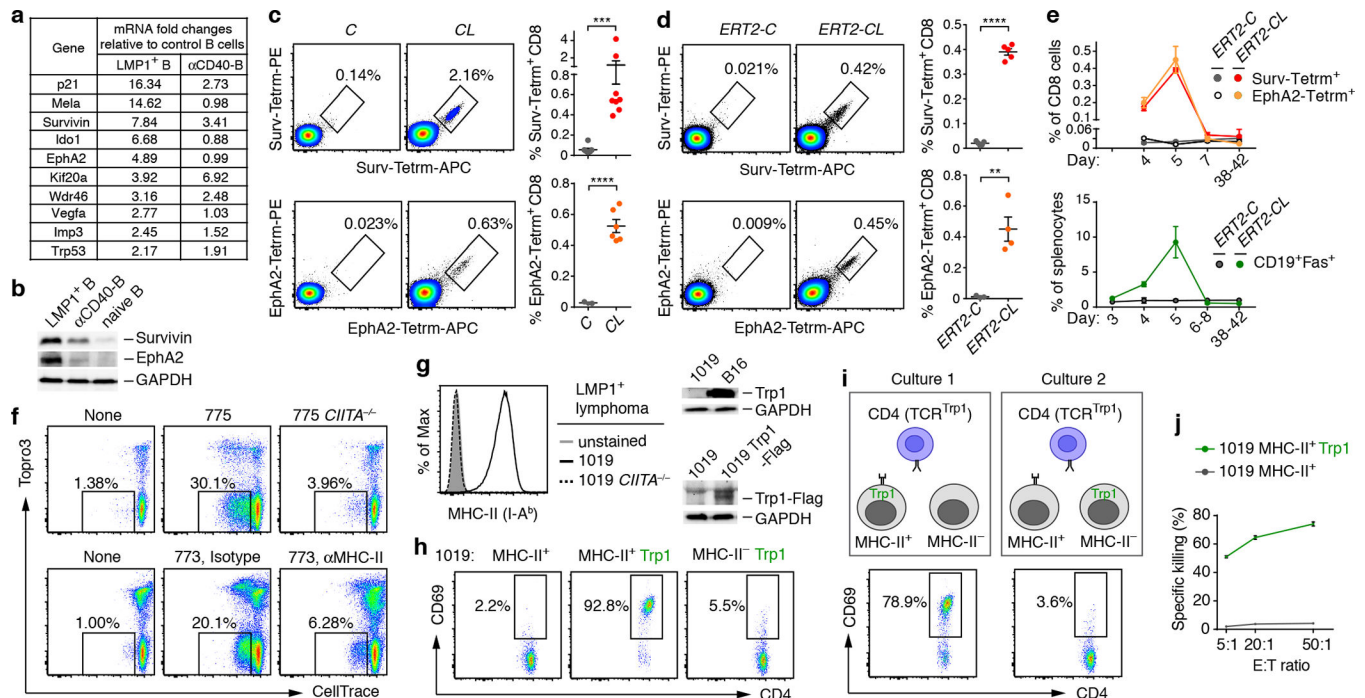


Fig. 2. LMP1-induced cellular antigens known as TAAs are targets of T cells.

a, Relative transcript levels of genes encoding known TAAs in LMP1⁺ and CD40-activated B cells compared to control B cells (see Methods). **b**, Immunoblots of Survivin and EphA2 in the indicated B cells. **c**, **d**, MHC-I tetramer (Tetrm) staining of CD8 cells specific for H-2D^b-restricted Survivin_{20–28} (Surv) epitope or H-2K^b-restricted EphA2_{682–689} epitope from spleens of 6-day-old *CL* mice (**c**) or *ERT2-CL* mice 5 days post-tamoxifen treatment (**d**), compared to the respective littermate controls (*C*, *CD19-cre*^{+/+}; *ERT2-C*, *CD19-cre*^{ERT2/+}). Left, representative FACS plots; right, summary data. Each circle represents one mouse. **e**, Dynamics of Surv-Tetrm⁺ and EphA2-Tetrm⁺ CD8 cells (upper) and LMP1⁺ B cells (lower, CD19⁺Fas⁺; Fas is used as a surrogate marker for LMP1 expression) analyzed by FACS in spleens of *ERT2-CL* mice and littermate controls over time after tamoxifen treatment. **f**, Proliferation of CD4 cells primed *in vitro* by LMP1⁺ B cells, in response to 775 that expresses or lacks MHC-II (upper) or 773 in the presence of MHC-II blocking antibody or isotype control (lower). **g**, Left panel, analysis of MHC-II (I-A^b) expression in 1019 and its *CIITA*^{-/-} subline. Right panel, immunoblotting of Trp1 or Trp1-Flag in 1019 untransfected or transfected with Trp1-Flag mRNA. B16-F10 melanoma cells served as positive control for Trp1 expression. **h**, CD69 expression on naive CD4 cells from Trp1 mice after co-culturing 18 h with 1019 (MHC-II⁺) or the *CIITA*^{-/-} (MHC-II⁻) subline transfected with Trp1 mRNA, or untransfected 1019 cells. **i**, Upper panel, scheme of strategy for assessing Trp1 MHC-II presentation pathways (see Methods). Lower panel, CD69 expression in CD4 cells of the indicated cultures. **j**, Cytotoxicity of Trp1-specific CD4 cells primed for 8 days *in vitro* by Trp1-transfected 1019 cells, against Trp1-transfected or untransfected 1019 cells. Error bars denote mean \pm s.e.m. All mice and cells are on the B6 background, except those in **c–e** (CB6F1).

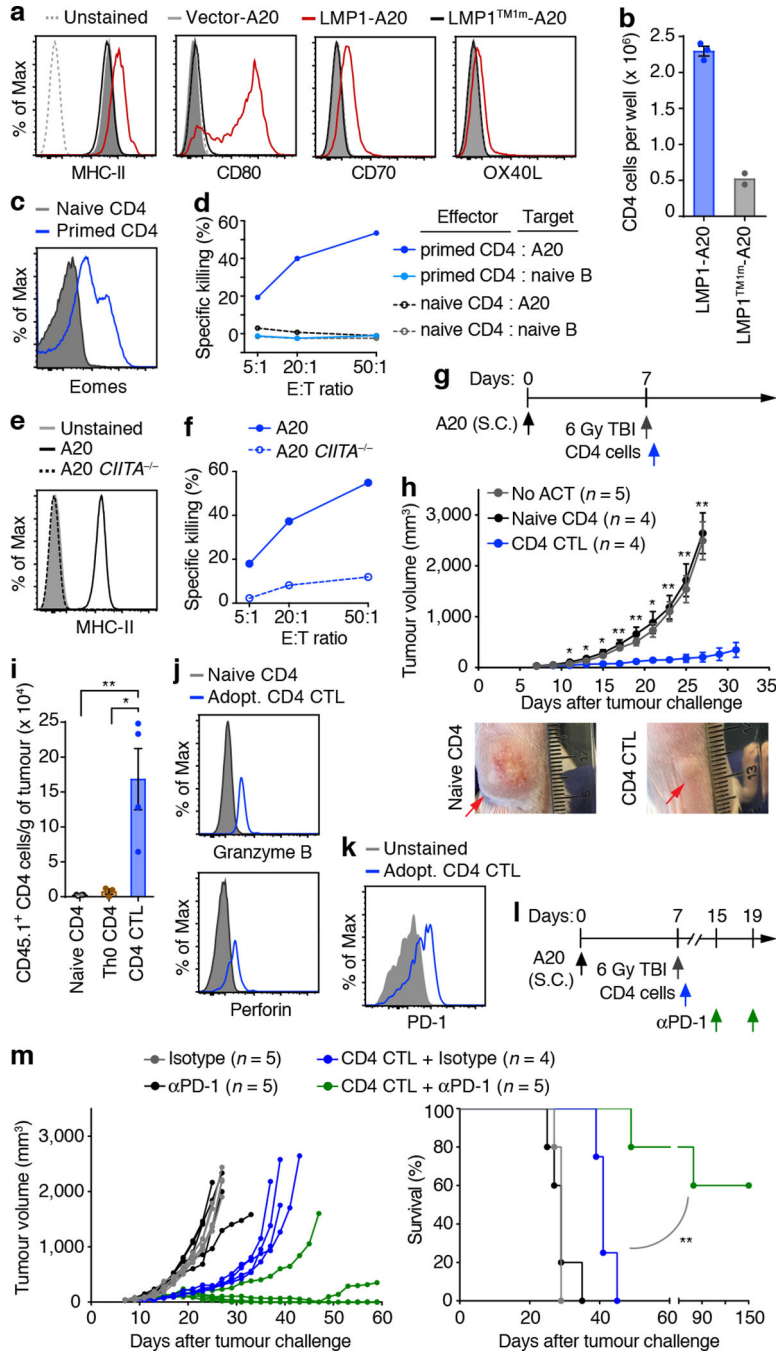


Fig. 3. Ectopically expressing LMP1 in murine tumour B cells enables generation of CD4 CTLs that target unmodified tumour B cells *in vitro* and *in vivo*.

a, FACS analysis of MHC-II and the indicated costimulatory ligands in A20 cells transduced with retroviral vectors expressing LMP1 or LMP1^{TM1m}, or an empty vector. Unstained vector-transduced cells served as negative control. **b**, Numbers of CD4 cells recovered after co-culturing naive CD4 cells (1×10^6) with LMP1- or LMP1^{TM1m}-transduced A20 cells for 6 days. **c**, Eomes levels in CD4 cells primed by LMP1-A20 cells as in **b**, compared to naive CD4 cells. Foxp3⁺ Tregs were excluded. **d**, Cytotoxicity of primed CD4 cells and naive CD4

cells against the indicated target cells. **e**, Analysis of MHC-II expression in A20 and A20 *CIITA*^{-/-} cells. **f**, Cytotoxicity of primed CD4 cells against A20 versus A20 *CIITA*^{-/-} cells. **g**, Schematic diagram of the ACT protocol (see Methods). TBI, preconditioning total body irradiation. **h**, Upper panel, mean tumour volumes in the indicated groups of mice treated as in **g**. Lower panel, representative pictures taken on day 27 of tumours in mice treated with the indicated CD4 cells. **i**, Numbers (per gram of tumour) of intra-tumoural adoptive CD4 cells (excluding Foxp3⁺ Tregs) recovered from A20-bearing mice (CD45.2⁺) receiving the indicated CD4 cells (CD45.1⁺), determined by FACS 8 days after adoptive transfer. **j**, Granzyme B and Perforin levels in intra-tumoural CD45.1⁺ adoptive CD4 cells recovered from CD4 CTL-treated mice as in **i**, compared to naive CD4 cells from normal mice. **k**, PD-1 expression on intra-tumoural adoptive CD4 cells as in **j**. **l**, Schematic diagram of the ACT protocol combined with PD-1 blockade (see Methods). **m**, Tumour volumes (left; each line represents an individual tumour) and survival (right) of A20-bearing mice treated as in **l**. Error bars denote mean ± s.e.m. All mice are on the BALB/c background.

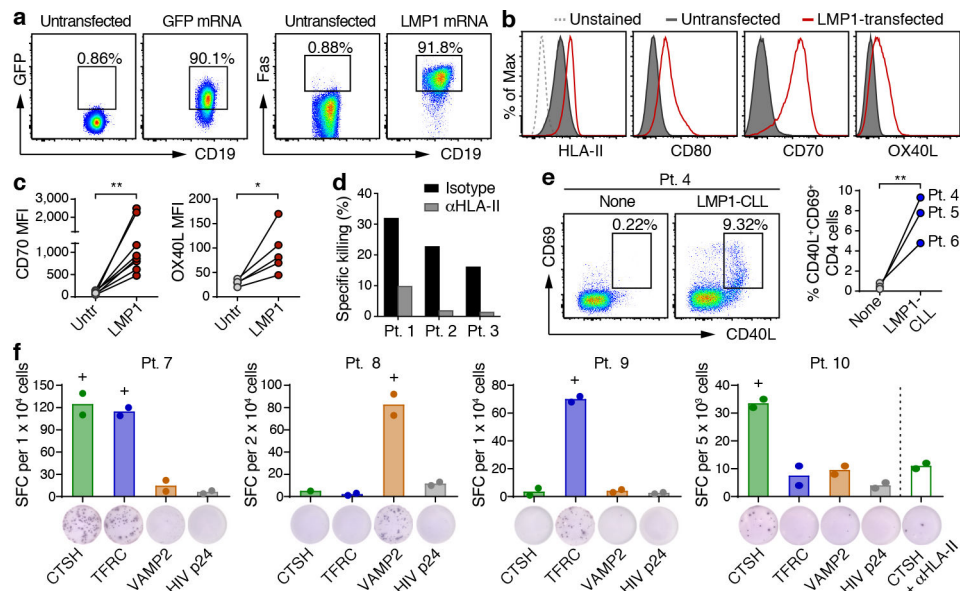


Fig. 4. Ectopically expressing LMP1 in patient tumour B cells enables generation of autologous CD4 CTLs targeting tumour antigens.

a, FACS analysis of transfection efficiency in patient CLL cells electroporated with GFP or LMP1 mRNA, assessed 2 days post-electroporation. Fas is used as a surrogate marker for LMP1 expression. **b**, FACS analysis of HLA-II and the indicated costimulatory ligands in LMP1-transfected versus untransfected CLL cells. Unstained CLL cells served as negative control in HLA-II analysis. **c**, Mean fluorescence intensities (MFI) of CD70 and OX40L in LMP1-transfected versus untransfected (Untr) CLL cells, assayed as in **b**. Each circle represents one patient. **d**, Cytotoxicity of autologous CD4 cells stimulated by LMP1-transfected CLL cells, against parental CLL cells at an E:T ratio of 25:1 in the presence of HLA-II blocking or isotype control antibody. Pt., patient. Unstimulated CD4 cells had no killing activity (data not shown). **e**, Co-expression of CD69 and CD40L on effector/memory CD4 cells from CLL patients after culturing 18 h with or without LMP1-transfected CLL cells (LMP1-CLL). Representative FACS plots are shown on the left and summary data on the right. **f**, IFN- γ ELISPOT responses of CD4 cells pre-stimulated with LMP1-CLL, against autologous dendritic cells pulsed with individual (CTSH₁₈₅₋₁₉₈) or pooled (TFRC₁₉₈₋₂₁₀ plus TFRC₆₈₀₋₆₉₃ or VAMP2₄₄₋₆₀ plus VAMP2₅₀₋₆₆) epitope peptides from the selected CLL TAAs. In Pt. 10, the assay was performed with or without HLA-II blocking antibody. An irrelevant HIV p24₁₆₄₋₁₈₁ peptide served as negative control. Numbers of spot-forming cells (SFC) in individual wells and their mean value per initial seeding number of CD4 cells are presented on the y-axis; representative ELISPOT images below the x-axis. +, positive ELISPOT response (see Methods).